2015

Control of plant stem cell function by conserved interacting transcriptional regulators

Yun Zhou

Xing Liu

Zachary L. Nimchuk

Eric M. Engstrom
William & Mary

Recommended Citation

Zhou, Yun; Liu, Xing; Nimchuk, Zachary L.; and Engstrom, Eric M., Control of plant stem cell function by conserved interacting transcriptional regulators (2015). *Nature*, 517(7534), 377-U528. https://doi.org/10.1038/nature13853

LETTER

doi:10.1038/nature13853

Control of plant stem cell function by conserved interacting transcriptional regulators

Yun Zhou[1], Xing Liu[1], Eric M. Engstrom[2]†, Zachary L. Nimchuk[1,3]†, Jose L. Pruneda-Paz[4], Paul T. Tarr[1], An Yan[1], Steve A. Kay[5] & Elliot M. Meyerowitz[1,3]

Plant stem cells in the shoot apical meristem (SAM) and root apical meristem are necessary for postembryonic development of aboveground tissues and roots, respectively, while secondary vascular stem cells sustain vascular development[1–4]. WUSCHEL (WUS), a homeodomain transcription factor expressed in the rib meristem of the *Arabidopsis* SAM, is a key regulatory factor controlling SAM stem cell populations[5,6], and is thought to establish the shoot stem cell niche through a feedback circuit involving the CLAVATA3 (CLV3) peptide signalling pathway[7]. WUSCHEL-RELATED HOMEOBOX 5 (WOX5), which is specifically expressed in the root quiescent centre, defines quiescent centre identity and functions interchangeably with WUS in the control of shoot and root stem cell niches[8]. WOX4, expressed in *Arabidopsis* procambial cells, defines the vascular stem cell niche[9–11]. WUS/WOX family proteins are evolutionarily and functionally conserved throughout the plant kingdom[12] and emerge as key actors in the specification and maintenance of stem cells within all meristems[13]. However, the nature of the genetic regime in stem cell niches that centre on *WOX* gene function has been elusive, and molecular links underlying conserved WUS/WOX function in stem cell niches remain unknown. Here we demonstrate that the *Arabidopsis* HAIRY MERISTEM (HAM) family of transcription regulators act as conserved interacting cofactors with WUS/WOX proteins. HAM and WUS share common targets *in vivo* and their physical interaction is important in driving downstream transcriptional programs and in promoting shoot stem cell proliferation. Differences in the overlapping expression patterns of WOX and HAM family members underlie the formation of diverse stem cell niche locations, and the HAM family is essential for all of these stem cell niches. These findings establish a new framework for the control of stem cell production during plant development.

To identify the molecular mechanism underlying WUS functions in stem cells, we screened for WUS-interacting transcription cofactors using yeast-two-hybrid assays with a transcription factor library[14], and found that HAIRY MERISTEM 1 (HAM1) strongly and specifically interacts with WUS (Fig. 1a). *HAM* genes, encoding GRAS domain transcription regulators, contribute to shoot stem cell function in *Petunia* and *Arabidopsis*[15–17]. Four *HAM* genes (*HAM1–HAM4*) have been identified in *Arabidopsis*[16], and further yeast assays revealed that WUS also interacted with three other HAM family members (Extended Data Fig. 1a). WUS–HAM associations were confirmed by bimolecular fluorescence complementation (BiFC) assays in tobacco (*Nicotiana benthamiana*), in which WUS and HAM were fused to the amino- and carboxy-terminal halves of green fluorescent protein (GFP), respectively (GFPn and GFPc). Strong GFP fluorescence in nuclei was observed when GFPn–WUS was co-transformed with GFPc–HAM (Fig. 1b, c and Extended Data Fig. 1b–e). WOX4 and WOX5 also interacted with HAM proteins in BiFC assays (Fig. 1d and Extended Data Fig. 1f–q). These WOX–HAM interactions were further confirmed through *in vitro* pull-down assays, where glutathione *S*-transferase (GST)–WOX4 but not GST bound HAM4–His_6, and GST–WUS but not GST bound HAM1–His_6 (Fig. 1e). Interactions *in planta* were then tested using co-immunoprecipitation assays in tobacco, in which WUS–GFP bound Flag–HAM1 (Fig. 1f) and Flag–HAM2 (Fig. 1g), GFP–WOX4 bound Flag–HAM4 (Fig. 1h), and WOX5–GFP bound Flag–HAM2 (Fig. 1i). In short, with multiple approaches, our work revealed physical interactions between HAM and WUS/WOX family members.

We next constructed various deleted derivatives of HAM1 and WUS for yeast two-hybrid assays to identify essential regions for their interactions. Deleting amino acids from 117 to 230 (D117–230) in HAM1 abolished the interaction (Extended Data Fig. 2a). This amino-terminal fragment is important for HAM1 function in stem cell maintenance, as HAM1(D117–230) did not complement the *ham1;2;4* early termination phenotype, whereas full-length HAM1 driven by the same *HAM1* promoter did (Extended Data Fig. 2b–g), and it is conserved in HAM proteins from *Arabidopsis* and across different plant species (Extended Data Fig. 2h–j). Deletion analyses of WUS identified a carboxy-terminal region required for interaction with HAM1 (Extended Data Fig. 3a), which is also required for WUS function (Extended Data Fig. 3b–d) and is conserved in different plant species (Extended Data Fig. 3e).

To dissect the roles of the HAM–WUS interaction in controlling shoot stem cell niches, genetic interactions were analysed between *ham1;2;3* (lacking the function of three of four *HAM* genes) and the weak *wus* allele *wus-7* (missense mutant), which forms a functional shoot apex[18] similar to wild type in terms of vegetative and inflorescence meristems (Fig. 2a, b, e). Different from *wus-7* single mutants (Fig. 2b) or *ham1;2;3* triple mutants (Fig. 2c), *wus-7;ham1;2;3* quadruple mutants display early termination of vegetative meristem development (Fig. 2d), thus resembling *wus* complete loss of function (null) mutants[5]. This effect also occurred in *wus-7/wus-7;ham1/ham1;ham2/ham2;ham3/+* plants, in which 41 out of 45 plants showed strong termination of inflorescence and floral meristems, with only leaves (Fig. 2h) or barren pedicels (flowers without carpels) (Fig. 2g) left at the top of the main shoot, a phenotype typical of *wus-1* null mutants[5], but never observed in *wus-7* (Fig. 2e) or *ham1/ham1;ham2/ham2;ham3/+* (Fig. 2f) plants. Secondary inflorescence meristems initiated from axillary meristems in *wus-7/wus-7;ham1/ham1;ham2/ham2;ham3/+* plants also terminated prematurely (Extended Data Fig. 4a, b). Additionally, three out of four *wus-7/wus-7;ham1/ham1;ham2/ham2;ham4/+* plants displayed inflorescence meristem termination and lacked carpels (Extended Data Fig. 4c). A dose-dependent enhancement of stem cell termination was evident in *wus-7;ham1/+;ham2/+;ham3/+* and *wus-7; ham1/+;ham2/ham2;ham3/ham3* backgrounds (Extended Data Fig. 4d–f), demonstrating a functional interdependence between WUS and HAM family members *in vivo*. Downregulation of *HAM1*, *HAM2* and *HAM3* in a *ham4* shoot meristem, through activation of the microRNA *MIR171*—reported to target the *HAM1*, *HAM2* and *HAM3* genes[19]—led to terminated vegetative development (Extended

[1]Division of Biology, California Institute of Technology, 1200 East California Boulevard, Pasadena, California 91125, USA. [2]Biology Department, College of William and Mary, Williamsburg, Virginia 23187-8795, USA. [3]Howard Hughes Medical Institute, California Institute of Technology, 1200 East California Boulevard, Pasadena, California 91125, USA. [4]Section of Cell and Developmental Biology, Division of Biological Sciences, University of California San Diego, La Jolla, California 92093, USA. [5]University of Southern California, Molecular and Computational Biology, Department of Biological Sciences, Dana and David Dornsife College of Letters, Arts and Sciences, Los Angeles, California 90089, USA. †Present addresses: Department of Biology, Rollins College, Winter Park, Florida 32789, USA (E.M.E.); Department of Biological Sciences, Latham Hall RM 408, Virginia Tech, 220 Ag Quad Lane, Blacksburg, Virginia 24061, USA (Z.L.N.).

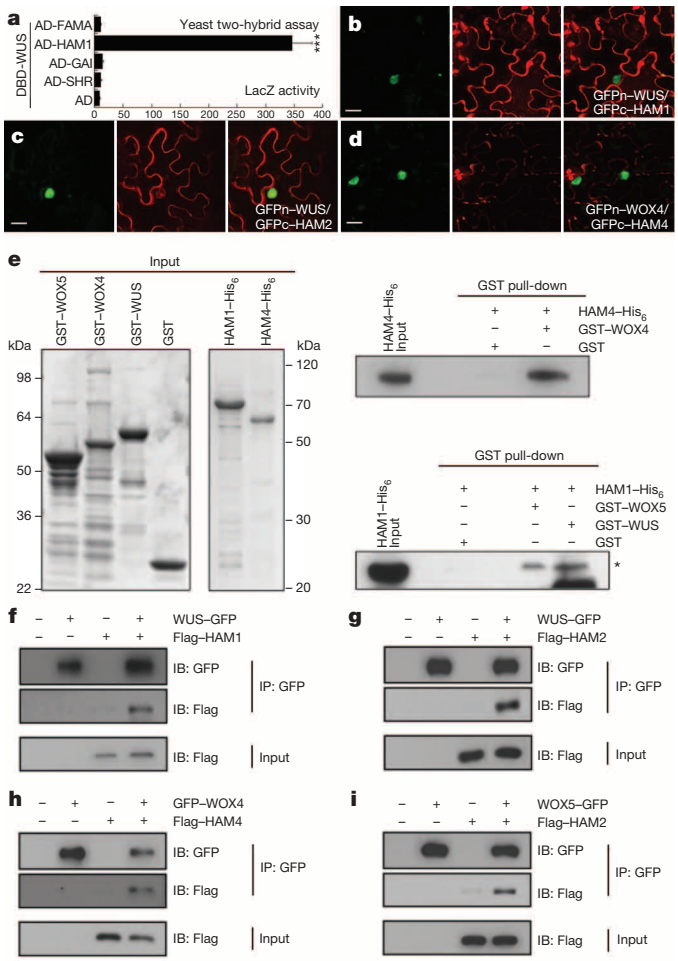

Figure 1 | WUS/WOX and HAM family proteins physically interact. **a**, LacZ activity in yeast two-hybrid assays. AD, activation domain; DBD, DNA-binding domain. Error bars show mean ± standard error of the mean (s.e.m.) ($n = 3$ biological replicates). ***$P < 0.001$ (two-tailed t-test). **b**–**d**, BiFC in tobacco. Panels (left to right): GFP; propidium iodide (PI) staining; merged channels. Scale bars, 20 μm. **e**, SDS–polyacrylamide gel electrophoresis (SDS–PAGE) of input recombinant proteins stained by Coomassie blue (left), and pull-down of His_6-tagged HAM proteins through GST-tagged WUS/WOX proteins detected by immunoblotting with anti-His antibody (right). Asterisk indicates HAM1–His_6 band and numbers indicate the apparent molecular weight of the protein bands in the protein standard. **f**–**j**, Co-immunoprecipitation of WUS–GFP and Flag–HAM1 (**f**), WUS–GFP and Flag–HAM2 (**g**), GFP–WOX4 and Flag–HAM4 (**h**), WOX5–GFP and Flag–HAM2 (**i**) (see Methods). IB, immunoblot; IP, immunoprecipitation.

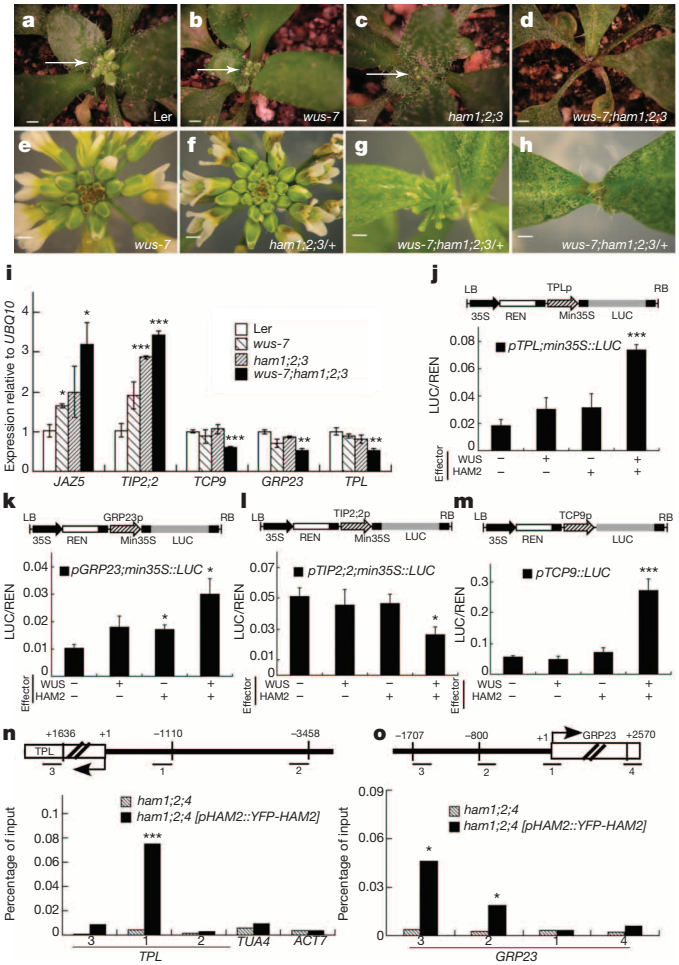

Figure 2 | *WUS* and *HAM* family genes cooperatively control the shoot stem cell niche and co-regulate a common gene set. **a**–**h**, Shoot apices (**a**–**d**) (arrows) and inflorescence structures (**e**–**h**) of plants of indicated genotypes (Ler, wild type). Scale bars, 2 mm. **i**, RT–PCR quantification of WUS and HAM target gene expression in indicated genotypes. Error bars show mean ± s.e.m. ($n = 3$ biological replicates). **j**–**m**, Ratio of firefly luciferase (LUC) to *Renilla* luciferase (REN) activity in tobacco cells co-transformed with different reporter constructs (structure above each graph) and indicated effectors (see Methods). Min35S, 60-base-pair 35S minimum element; LB, transfer DNA (T-DNA) left border; RB, T-DNA right border. Error bars show mean ± s.e.m. ($n = 3$ biological replicates). **n**, **o**, ChIP of HAM2 protein with *TPL* or *GRP23* chromatin regions, with amplicon locations (bars with numbers) shown above each graph. The ChIP experiments were repeated three times using independent biological replicates with similar results, and one representative data set is shown. **i**–**o**, *$P < 0.05$, **$P < 0.01$, ***$P < 0.001$ (two-tailed t-test).

Data Fig. 4g, h) similar to the *wus-1* phenotype, suggesting that WUS alone is not sufficient to maintain SAMs in the absence of *HAM* activity. Finally, the *wus-1;ham1;2;3* quadruple homozygote resembles a *wus-1* single mutant in several aspects including the vegetative meristem (Extended Data Fig. 4i–l), suggesting that *WUS* and *HAM* genes could act together at the SAM. All these genetic data are consistent with the hypothesis that WUS and HAM function as partners in shoot meristem maintenance.

In addition to genetic interactions, the molecular function of the WUS–HAM interaction was further investigated. First, quantitative PCR with reverse transcription (RT–PCR) results (Fig. 3i) demonstrated that HAM proteins regulate expression of a set of genes including *JAZ5*, *TIP2;2*, *TCP9*, *GRP23* and *TPL*, which were reported to be directly regulated by WUS[20]. These WUS downstream targets were misregulated in *wus-7* or *ham1;2;3* triple mutants in similar manners, and *wus-7* and *ham1;2;3* synergistically regulated their expression (Fig. 2i), consistent with functional physical (Fig. 1) and genetic (Fig. 2a–h) interactions between WUS and HAM. Second, dual luciferase assays were conducted *in planta* to confirm the direct effects of WUS–HAM on target gene expression. Compared with empty-vector controls, the target genes examined were moderately (Fig. 2j–k) or barely (Fig. 2l, m) regulated by WUS or HAM alone, but were markedly affected when WUS and HAM were combined (Fig. 2j–l), indicating a role for the WUS–HAM interaction in regulating their transcription activities. Last, chromatin immunoprecipitation (ChIP) experiments demonstrated an *in vivo* association of yellow fluorescent protein (YFP)–HAM2 proteins with *TPL* (Fig. 2n) and *GRP23* promoters (Fig. 2o), genomic regions similar to those reported to associate with WUS protein *in vivo*[20], supporting the notion that HAM family members are functional WUS cofactors in controlling the shoot stem cell niche through regulation of common target genes.

Consistently with physical and genetic interactions between HAM and WOX members, visualization of *HAM* and *WUS/WOX* fluorescent

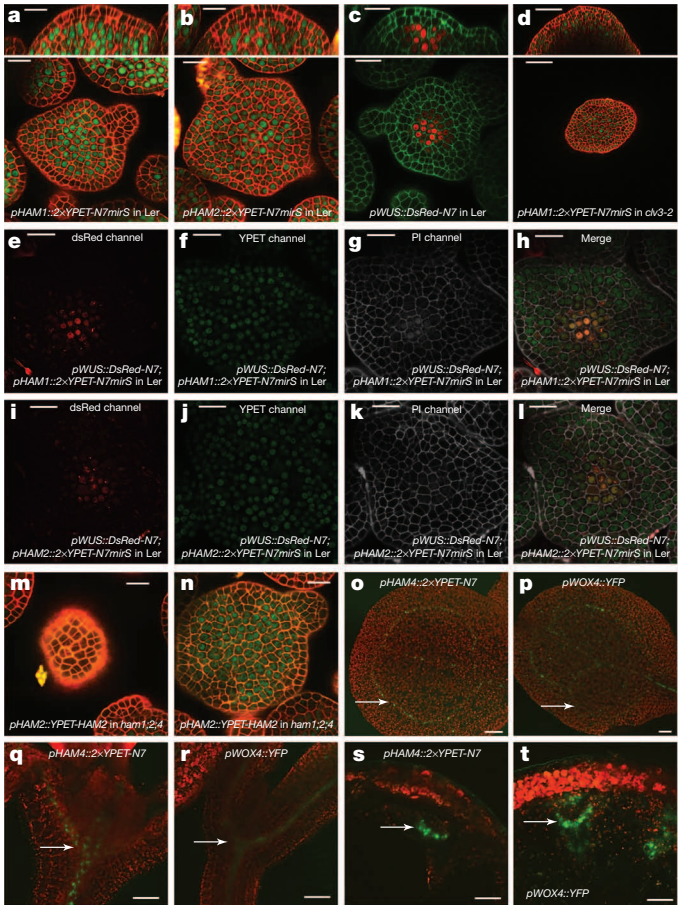

Figure 3 | *HAM* and *WUS*/*WOX* expression domains overlap. **a**–**d**, Expression of *pHAM1::2×YPET-N7MICRORNASENSITIVE* marker (*pHAM1::2×YPET-N7mirS*) (green) (**a**), *pHAM2::2×YPET-N7mirS* (green) (**b**), *pWUS::DsRed-N7* (red) (**c**) in Ler inflorescence meristem, and *pHAM1::2×YPET-N7mirS* (green) marker in a *clv3-2* inflorescence meristem (**d**). Orthogonal (top) and transverse section (bottom) views of the same plant are shown. **e**–**l**, Overlapping expression patterns of *pWUS::DsRed-N7* with *pHAM1::2×YPET-N7mirS* or *pHAM2::2×YPET-N7mirS* in the same shoot meristems (see Methods). Panels (from left to right): dsRed (red); YPET, an improved version of YFP (green); PI (grey); merged channels. **m**, **n**, Expression of *pHAM2::YPET-HAM2* translational marker (green) in L1 (**m**) and L3 (**n**) of the same *ham1;2;4* SAM. **o**–**t**, Overlapping expression patterns of *pHAM4::2×YPET-N7* and *pWOX4::YFP* (green, arrows) in the provascular and procambium cells in cotyledons (**o**, **p**), seedlings (**q**, **r**), and stem transverse sections (**s**, **t**). PI counterstain: red (**a**, **b**, **d**, **m**, **n**); green (**c**); grey (**g**, **h**, **k**, **l**). Chlorophyll autofluorescence: red (**o**–**t**). Scale bars: 50 μm (**d**, **s**, **t**); 200 μm (**o**); 100 μm (**p**–**r**); 20 μm (**a**–**c**, **e**–**n**).

transcriptional reporters revealed that WOX and HAM family expression overlapped *in planta*. In vegetative (Extended Data Fig. 5c–h) and inflorescence meristems (Fig. 3a–c), *HAM1* and *HAM2* expression overlapped with that of *WUS* in the rib meristem. *HAM1* is expressed in the rib meristem and peripheral zone but not in the L1 or L2 layers of the central zone (Fig. 3a and Supplementary Video 1), while *HAM2* expression peaks within the centre of the rib meristem (Fig. 3b). Similarly to *WUS* (Extended Data Fig. 5a, b), *HAM1* is negatively controlled by *CLV* signalling, as *HAM1* is expressed throughout *clv3-2* meristems (Fig. 3d). We imaged the *WUS* and *HAM1* or *HAM2* reporters in the same SAMs (Fig. 3e–l). Although expressed broadly, signals from *HAM1* (Fig. 3f) or *HAM2* (Fig. 3j) overlap with *WUS* signals (Fig. 3e, i) in the same rib zone cells (Fig. 3h, l and Extended Data Fig. 5i–p). As the WUS protein has been reported to move in the SAM from its site of transcription in the rib domain[21], the WUS and HAM1/HAM2 interaction domain in SAMs could be broader than their transcriptional domain overlap. We also examined the HAM2 translational reporter *pHAM2::YPET-HAM2* in the *ham1;2;4* SAM (Fig. 3m, n and Extended Data Fig. 6), which completely complements the *ham1;2;4* triple mutant (Extended Data Fig. 6a–c), and it showed a pattern similar to the HAM2 transcriptional reporter: a strong signal in the centre starting from L3 and low or no signal in the L1 layer (Fig. 3m, n and Extended Data Fig. 6d, e). Taken together, the co-localization of WUS and HAM1/HAM2 in SAMs is consistent with functional WUS–HAM1/HAM2 interactions (Figs 1 and 2).

HAM4 and *WOX4* are co-expressed in the provascular or procambial cell types of various tissues (Fig. 3o–t and Extended Data Fig. 7). In stem transverse sections, *HAM4* is expressed specifically in the procambium, overlapping with *WOX4* expression, as well as with the *HAM3* and *HAM1* expression domains (Fig. 3s, t and Extended Data Fig. 7j–l). The tightly co-regulated spatial and temporal *HAM4* and *WOX4* expression patterns are consistent with a WOX4–HAM4 interaction module (Fig. 1h). Both *HAM2* transcriptional and translational reporters (Extended Data Fig. 8) are expressed in root meristem cells including the quiescent centre, overlapping with the quiescent-centre-specific *WOX5* expression domain[8], consistent with previous reports from cell-type-specific transcriptome analyses[22,23] and indicating the possibility of WOX5–HAM2 interactions in roots. Our finding that both WUS and WOX5 interact with HAM2 may be partially accounted for by the fact that WUS and WOX5 are interchangeable in controlling SAMs and root apical meristems[8]. Taken together, distinct and overlapping expression patterns of *HAM* and *WOX* members indicate that specific HAM–WOX pairs function within different stem cell niches throughout the plant.

To address the importance of the entire HAM family in the control of stem cell niches, we generated a *ham1;2;3;4* quadruple homozygous mutant. Compared with wild type, *ham1;2;3;4* plants displayed growth arrest at the early seedling stage, containing short roots and terminated shoots with two small leaf-like structures 26 days after germination (DAG) (Fig. 4a–c and Extended Data Fig. 9a–d); the shoot apices exhibited valley-like shapes at 26 DAG, lacking functional meristems (Fig. 4d); the hypocotyl transverse sections showed clear vascular defects, and the vascular bundles had reduced numbers of xylem vessels, fibres (dark-blue-stained) and phloem cells (red-stained), consistent with a reduction in the stem cell activity necessary for generating these cell types (Fig. 4e, f). Moreover, mid-veins in *ham1;2;3;4* leaf-like tissues did not differentiate but instead accumulated a dark-staining cell mass, resembling ground tissue cells (Extended Data Fig. 9e, f). This is similar to, but much stronger than, the reported *WOX4* RNA interference phenotype[10]. Root meristematic activity is also severely compromised in *ham* multiple mutants. The quiescent centre and columella stem cells (CSCs) in *ham1;2;3;4* mutants displayed enlarged and irregular shapes (Extended Data Fig. 9g, h) and, with incomplete penetrance, the CSCs in *ham1;2;3* mutants differentiate (Extended Data Fig. 9i–l), resembling reported defects in *wox5* mutants[8]. However, the root phenotype of *ham1;2;3* or

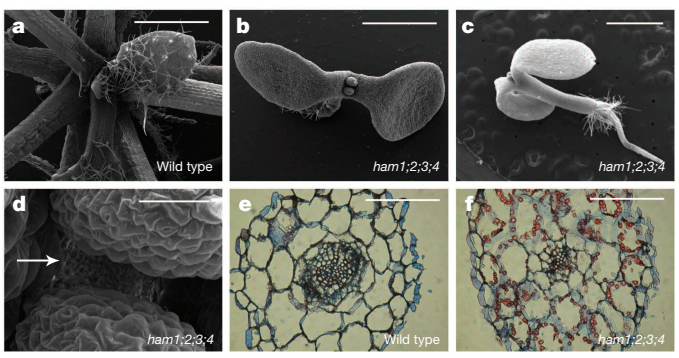

Figure 4 | HAM family members are essential for various plant stem cell activities. Scanning electron microscopic imaging of wild-type (**a**) and *ham1;2;3;4* (**b**–**d**) seedlings (26 DAG). Arrow indicates a *ham1;2;3;4* plant lacking a functional SAM. **e**, **f**, Transverse sections of wild-type and *ham1;2;3;4* hypocotyls (7 DAG). Scale bars: 1 mm (**a**–**c**, **e**, **f**); 50 μm (**d**).

ham1;2;3;4 plants is much more severe than that of the *wox5* mutant, suggesting that HAM regulates root meristem development not only through direct interaction with WOX5 but also through WOX5-independent pathways. In summary, in diverse meristems, *ham1;2;3;4* mutants display defects that share similarities with mutants lacking WOX activities, supporting the idea that HAM proteins are cofactors for WUS/WOX-family-mediated stem cell niche maintenance. Given the evolutionary conservation of plant meristem cell niches and the *WOX*/*HAM* gene families[12,16], and the fact that WOX–HAM interactions exist in flowering plants besides *Arabidopsis* (Extended Data Fig. 10), this work establishes a new basis for studying stem cell niches in *Arabidopsis*, and provides a paradigm for meristem cell control regimes likely to be universal in flowering plants.

Online Content Methods, along with any additional Extended Data display items and Source Data, are available in the online version of the paper; references unique to these sections appear only in the online paper.

Received 25 February; accepted 10 September 2014.
Published online 26 October 2014.

1. Meyerowitz, E. M. Genetic control of cell division patterns in developing plants. *Cell* **88,** 299–308 (1997).
2. Sablowski, R. The dynamic plant stem cell niches. *Curr. Opin. Plant Biol.* **10,** 639–644 (2007).
3. Miyashima, S., Sebastian, J., Lee, J. Y. & Helariutta, Y. Stem cell function during plant vascular development. *EMBO J.* **32,** 178–193 (2012).
4. Dinneny, J. R. & Benfey, P. N. Plant stem cell niches: standing the test of time. *Cell* **132,** 553–557 (2008).
5. Laux, T., Mayer, K. F., Berger, J. & Jurgens, G. The *WUSCHEL* gene is required for shoot and floral meristem integrity in *Arabidopsis*. *Development* **122,** 87–96 (1996).
6. Mayer, K. F. *et al.* Role of *WUSCHEL* in regulating stem cell fate in the *Arabidopsis* shoot meristem. *Cell* **95,** 805–815 (1998).
7. Schoof, H. *et al.* The stem cell population of *Arabidopsis* shoot meristems in maintained by a regulatory loop between the *CLAVATA* and *WUSCHEL* genes. *Cell* **100,** 635–644 (2000).
8. Sarkar, A. K. *et al.* Conserved factors regulate signalling in *Arabidopsis thaliana* shoot and root stem cell organizers. *Nature* **446,** 811–814 (2007).
9. Hirakawa, Y., Kondo, Y. & Fukuda, H. TDIF peptide signaling regulates vascular stem cell proliferation via the *WOX4* homeobox gene in *Arabidopsis*. *Plant Cell* **22,** 2618–2629 (2010).
10. Ji, J. *et al.* WOX4 promotes procambial development. *Plant Physiol.* **152,** 1346–1356 (2010).
11. Suer, S., Agusti, J., Sanchez, P., Schwarz, M. & Greb, T. WOX4 imparts auxin responsiveness to cambium cells in *Arabidopsis*. *Plant Cell* **23,** 3247–3259 (2011).
12. Nardmann, J., Reisewitz, P. & Werr, W. Discrete shoot and root stem cell-promoting WUS/WOX5 functions are an evolutionary innovation of angiosperms. *Mol. Biol. Evol.* **26,** 1745–1755 (2009).
13. van der Graaff, E., Laux, T. & Rensing, S. A. The WUS homeobox-containing (WOX) protein family. *Genome Biol.* **10,** 248 (2009).
14. Pruneda-Paz, J. L. *et al.* A genome-scale resource for the functional characterization of *Arabidopsis* transcription factors. *Cell Rep.* **8,** 622–632 (2014).
15. Stuurman, J., Jaggi, F. & Kuhlemeier, C. Shoot meristem maintenance is controlled by a *GRAS*-gene mediated signal from differentiating cells. *Genes Dev.* **16,** 2213–2218 (2002).
16. Engstrom, E. M. *et al.* *Arabidopsis* homologs of the petunia hairy meristem gene are required for maintenance of shoot and root indeterminacy. *Plant Physiol.* **155,** 735–750 (2011).
17. Schulze, S., Schafer, B. N., Parizotto, E. A., Voinnet, O. & Theres, K. *LOST MERISTEMS* genes regulate cell differentiation of central zone descendants in *Arabidopsis* shoot meristems. *Plant J.* **64,** 668–678 (2010).
18. Graf, P. *et al.* *MGOUN1* encodes an *Arabidopsis* type IB DNA topoisomerase required in stem cell regulation and to maintain developmentally regulated gene silencing. *Plant Cell* **22,** 716–728 (2010).
19. Llave, C., Xie, Z., Kasschau, K. D. & Carrington, J. C. Cleavage of *Scarecrow-like* mRNA targets directed by a class of *Arabidopsis* miRNA. *Science* **297,** 2053–2056 (2002).
20. Busch, W. *et al.* Transcriptional control of a plant stem cell niche. *Dev. Cell* **18,** 841–853 (2010).
21. Yadav, R. K. *et al.* WUSCHEL protein movement mediates stem cell homeostasis in the *Arabidopsis* shoot apex. *Genes Dev.* **25,** 2025–2030 (2011).
22. Nawy, T. *et al.* Transcriptional profile of the *Arabidopsis* root quiescent center. *Plant Cell* **17,** 1908–1925 (2005).
23. Brady, S. M. *et al.* A high-resolution root spatiotemporal map reveals dominant expression patterns. *Science* **318,** 801–806 (2007).

Supplementary Information is available in the online version of the paper.

Acknowledgements The authors are grateful to R. Deshaies for his support with the protein purification and pull-down experiments, to D. Rees for sharing the 96-well format luminometer, to T. Laux, T. Greb and X. Deng for sharing published reagents, to K. Sugimoto and A. Roeder for help with the histology experiments and critical reading of the manuscript, to A. Sampathkumar for the suggestion of confocal imaging, and to A. Garda and L. Wang for technical support. Scanning electron microscopy was performed at the Applied Research Center of the College of William and Mary with technical assistance from B. Robertson. This work was funded by National Institutes of Health (NIH) grant R01 GM104244 and by the Howard Hughes Medical Institute and the Gordon and Betty Moore Foundation (through grant GBMF3406) to E.M.M., by a Caltech Gosney Postdoctoral Fellowship to Y.Z., by NIH grants GM094212, GM056006 and GM067837 to S.A.K., and was aided by a grant from The Jane Coffin Childs (JCC) Memorial Fund for Medical Research to X.L., a JCC fellow.

Author Contributions Y.Z. and E.M.M. conceived the experiments. Y.Z., X.L., E.M.E. and A.Y. performed experiments. J.L.P.-P. and S.A.K. provided the transcription factor library. Z.L.N. and P.T.T. contributed reagents. Y.Z., X.L. and A.Y. analysed data. Y.Z. and E.M.M. wrote the manuscript and X.L., Z.L.N. and A.Y. revised it. All authors read and approved the manuscript.

Author Information Reprints and permissions information is available at www.nature.com/reprints. The authors declare no competing financial interests. Readers are welcome to comment on the online version of the paper. Correspondence and requests for materials should be addressed to E.M.M. (meyerow@caltech.edu).

METHODS

Plant materials and growth conditions. *Arabidopsis thaliana* plants were grown in a sunshine soil/vermiculite/perlite mixture under continuous light at 20 °C. The mutant lines *ham1;2;3* (triply homozygous for mutant alleles of *ham1-1*, *ham2-1* and *ham3-1*), *ham1;2;4* (triply homozygous for mutant alleles of *ham1-1*, *ham2-1* and *ham4-1*), *wus-7*, *wus-1*, *clv3-2* were previously described[5,16,18,24]. *wus-7;ham1;2;3*, *wus-7;ham1;2;4*, *wus-1;ham1;2;3*, and *ham1;2;3;4* mutants were generated through genetic crosses, and identified based on PCR genotyping in the F2 segregating population. Different mutant combinations in an *er* background were chosen for genetic and morphological analyses. All of the phenotypes were confirmed from multiple independent segregation lines to control for differences in ecotype background. PCR genotyping was performed as previously described[16,18]. Reporter lines for *pWUS::DsRed-N7* and *pWOX4::YFP* were previously reported[11,25].

Yeast two-hybrid assay. Yeast transformation and β-galactosidase assays were performed following the manufacturer's instructions (Clontech). Full-length cDNAs for *WUS*, *HAM1*, *HAM2*, *HAM3* and *HAM4* were cloned into pENTR/D/TOPO or pCR8 (Invitrogen), and then *WUS* cDNA was Gateway cloned to pDEST32, and *HAM1*, *HAM2*, *HAM3* and *HAM4* cDNAs were Gateway cloned into pDEST22 using standard LR reactions (Invitrogen). All of the deletion derivatives for WUS or HAM1 were generated through overlapping PCR with the primers listed later, cloned into pENTR/D-TOPO or pCR8, and cloned into pDEST32 or pDEST22 through LR recombination (Invitrogen). All clones were sequenced to confirm that they were in-frame and with designed deletions before being transformed into yeast. The bait and prey vectors were transformed into yeast strain MaV203, and three single transformed colonies per genotype were used as triplicate for the LacZ liquid assay in 96 Deepwell plates (Thermo) and optical density (OD) readings were recorded in a 96-well plate reader (Tecan). LacZ activity was calculated as $(OD_{420}\ \text{nm} \times 1{,}000)/(OD_{600}\ \text{nm} \times \text{cell volume in } \mu\text{l} \times \text{assay time in minutes})$ following the yeast two-hybrid handbook (Clontech), including a standard error from three biological replicates.

BiFC. For BiFC experiments, full-length *Arabidopsis WUS*, *WOX4*, *WOX5*, *HAM1*, *HAM2*, *HAM3*, *HAM4*, *BARD1* and *FAMA* cDNA Gateway clones were recombined into vectors containing each half of GFP (N or C terminus) to generate the fusion proteins (GFPn–WUS, GFPn–WOX4, GFPn–WOX5, GFPn–BARD1, GFPn–FAMA, GFPc–HAM1, GFPc–HAM2, GFPc–HAM3, GFPc–HAM4, GFPc–BARD1, GFPc–FAMA) as previously described[26]. Plasmid pairs for testing the specific interactions (such as GFPn–WUS and GFPc–HAM1) were co-transformed together with the P19 silencing suppressor[27] into *N. benthamiana* leaves through *Agrobacterium* infiltration. The infiltrated tobacco leaves were stained with PI and imaged using a Zeiss LSM 510 Meta confocal microscope two days after infiltration. Green GFP signals in nuclei (which demonstrate the physical interaction) and red PI staining signals (which indicate tobacco cell structure) were captured at the same time from different detection channels. A 488 nm laser line was used to stimulate GFP and PI. A 505–530 bandpass filter was used to collect GFP signal and a 585–615 bandpass filter was used to collect PI signal. BARD1, a nuclear-localized protein, was included as a negative control. FAMA, a bHLH transcription factor that has been demonstrated to interact with bHLH transcription factors[28], was used as an additional negative control. The positive signals for each pair were confirmed with four independent biological replicates, and representative images are shown in the figures. The same method was also used for tomato (*Solanum lycopersicum*) proteins, including GFPn–tomato WUS, GFPn–tomato WOX4 and GFPc–tomato HAM.

Co-immunoprecipitation and western blot analysis. *WUS* or *WOX5* cDNA in pCR8 was recombined to pMDC83 (ref. 29) to generate a WUS–GFP or WOX5–GFP fusion clone. Flag–HAM1, Flag–HAM2 and Flag–HAM4 were PCR amplified with primers 5′-CACCATGgactacaaggacgacgatgacaagggcggtggaagtCCCTTATCCTTTGAAAGGTTTCAAGG -3′, 5′-CTAACATTTCCAAGCAGAGACAGTAACAAGTTC-3′, and with primers 5′-CACCATGgactacaaggacgacgatgacaaggcggcggtggaagtCCCCTGCCCTTTGAGCAATTT-3′, 5′-TTAACATTTCCAAGCTGAGACAGTA-3′, and with primers 5′-CACCATGgactacaaggacgacgatgacaagggcggtggaagtAAAATCCCTGCATCATCTCCTC-3′, 5′-CTAAAACCGCCAAGCTGATGTGGCAACAAG-3′, respectively (lower-case letters indicate coding sequences for Flag and a linker). *GFP* DNA was amplified and sub-cloned in front of *WOX4* cDNA in-frame to generate a GFP–WOX4 fragment. Flag–HAM1, Flag–HAM2, Flag–HAM4 and GFP–WOX4 were then recombined into pMDC32 (ref. 29). For co-immunoprecipitation of WUS–GFP with Flag–HAM1, WUS–GFP with Flag–HAM2, GFP–WOX4 with Flag–HAM4, or WOX5–GFP with Flag–HAM2 in *N. benthamiana*, the constructs were introduced into *N. benthamiana* leaves through *Agrobacterium* infiltration. The leaves were harvested 2 days after infiltration and frozen in liquid nitrogen. For the immunoprecipitation of YFP–HAM2 in *Arabidopsis*, the shoot apices from the transgenic plants *pHAM2::YFP-HAM2* in *ham1;2;4* were harvested. The nuclei from *Arabidopsis* or tobacco were isolated, and then lysed with RIPA buffer (50 mM Tris-HCl, pH 7.5, 150 mM NaCl, 1% NP-40, 0.5% sodium deoxycholate, 0.1% SDS, 3 mM dithiothreitol (DTT), 2 mM NaF and 1 mM $NaVO_3$, or 50 mM Tris-HCl, pH 8.0, 150 mM NaCl, 1% NP-40, 0.5% sodium deoxycholate, 0.1% SDS for co-immunoprecipitation of GFP–WOX4 with Flag–HAM4) containing protease inhibitor cocktail (Roche) and 200 μM PMSF by incubation on ice for 30 min followed by brief sonication. Clear lysates were mixed with diluting buffer containing PMSF and protease inhibitor cocktail (50 mM Tris-HCl, pH 7.5, 150 mM NaCl, 3 mM DTT, 2 mM NaF and 1 mM $NaVO_3$, or 50 mM Tris-HCl, pH 8.0, 60 mM NaCl for co-immunoprecipitation of GFP–WOX4 with Flag–HAM4) (1:5, v:v), immunoprecipitated with GFP–Trap agarose beads (ChromoTek), and the beads were washed three times with the diluting buffer in spin columns (BioRad). The recovered proteins were eluted from the beads by boiling in 2× SDS sample buffer, separated by SDS–PAGE and transferred to nitrocellulose membrane (Millipore). Proteins were detected using anti-GFP antibody (Roche, catalogue #11814460001), anti-Flag antibody (Sigma, catalogue #F1804), and horseradish peroxidase (HRP)-conjugated anti-mouse antibody (Promega, catalogue #W4021). The co-immunoprecipitation experiments were repeated twice with similar results.

Protein expression constructs and protein purification. *WOX4* cDNA was amplified with primers 5′-CATA**GAATTC**ATGAAGGTTCATGAGTTTTCGAA-3′ and 5′-AGTT**GCGGCCGC**TCATCTCCCTTCAGGATGGAGAGGA-3′ (restriction enzyme sites are in bold), and cloned in-frame in pGEX-4T-1 with EcoRI and NotI sites. *WOX5* cDNA was amplified with primers 5′-ATTT**CCCGGG**TATGTCTTTCTCCGTGAAAGGTCG-3′ and 5′-AGTT**GCGGCCGC**TTAAAGAAAGCTTAATCGAAGATCT-3′ (restriction enzyme sites are in bold), and cloned in-frame in pGEX-4T-1 with XmaI and NotI sites. *WUS* cDNA was amplified with primers 5′-CATA**GAATTC**ATGGAGCCGCCACAGCATCAG-3′ and 5′-AGTT**GCGGCCGC**CTAGTTCAGACGTAGCTCAAGA-3′ (restriction enzyme sites are in bold), and cloned in-frame in pGEX-4T-1 with EcoRI and NotI sites. HAM1–His_6 tag was generated from PCR with primers 5′-CATA**GAATTC**ATGCCCTTATCCTTTGAAAGGTTTCAAGG-3′ and 5′-AGTT**GCGGCCGC**CTAGTGATGATGATGATGACATTTCCAAGCAGAGACAGTAACAAGTTCTT-3′ (restriction enzyme sites are in bold, and His_6 coding sequence is underlined), and cloned in-frame with thrombin cutting site in pGEX-4T-1 with EcoRI and NotI. HAM4–His_6 tag was generated from PCR with primers 5′-CATA**GAATTC**ATGAAAATCCCTGCATCATCTCCTC -3′ and 5′-AGTT**GCGGCCGC**CTAGTGATGATGATGATGAAACCGCCAAGCTGATGTGGCAACAAG-3′ (restriction enzyme sites are in bold, and His_6 coding sequence is underlined), and cloned in-frame with thrombin cutting site in pGEX-4T-1 with EcoRI and NotI. All proteins were expressed in Rosetta *Escherichia coli* (Novagen) by inducing with 0.4 mM isopropyl-β-D-thiogalactoside (IPTG) at 16 °C for 2–4 h. GST–WOX4, GST–WOX5 and GST were purified on glutathione resin. HAM1 was purified on glutathione resin followed by digestion with thrombin and chromatography on S200 resins as described previously[30,31]. HAM4 was purified on glutathione resin followed by digestion with thrombin and removal of the GST associated with glutathione resin as described previously[31].

***In vitro* pull-down assay.** GST–WOX4, GST–WOX5, GST–WUS or GST were immobilized on glutathione resin and incubated with HAM1–His_6 or HAM4–His_6 for 30 min at 4 °C. The glutathione resin was then washed three times and processed for SDS–PAGE analysis and western blot analysis using antibody to His-tag (Qiagen, catalogue #34660). The pull-down experiments were repeated twice with similar results.

Transactivation assay in tobacco. A 60 base pair (bp) minimal 35S fragment (the −60 minimal promoter) was amplified and cloned with BamHI/NcoI sites into the pGREEN800II LUC[32] to generate a pGREEN800II-60LUC. *TPL* promoter was PCR amplified from Col-0 genomic DNA with primers 5′-AACA**GGTACC**GAACGCTTCGTTTCATTAGTTTATC-3′ and 5′-AATA**GGATCC**GTTTTCTCTCACTTCCTTAAAAGACT-3′ (restriction enzyme sites are in bold) and cloned with KpnI/BamHI sites into the pGREEN800II-60LUC. *TIP2;2* promoter was amplified with primers 5′-AACA**GGTACC**CGAGTGAAGCAGATTGGGAGAGAA-3′ and 5′-AATA**CTGCAG**TTTGATCCGACAAAATAACTCTGTT-3′ and cloned with KpnI/PstI sites into the pGREEN800II-60LUC. *GRP23* promoter was amplified with primers 5′-AACA**GGTACC**CAGGTGTGATTGTCAATAGACTACG-3′ and 5′-AACA**GATATC**GGTGGAGGGAAAATGATTTAGGGTT-3′ and cloned with KpnI/EcoRV sites into the pGREEN800II-60LUC. *TCP9* promoter was amplified with primers 5′-AACA**GGTACC**GTATGCTGATGGTAGGCAAAAGTT-3′ and 5′-AATA**CTGCAG**TAAAATATAGCTGAGAGAAAACG-3′ and cloned with KpnI/PstI sites into the pGREEN800II LUC. The different reporter constructs (dual-luciferase reporter with different gene promoters) and indicated effectors (empty effector vector or WUS or HAM2, or WUS together with HAM2) were introduced into *N. benthamiana* leaves through *Agrobacterium* infiltration. The activities of LUC and REN were quantified 2 days after infiltration with a Dual Luciferase Assay kit (Promega), and luminescence was recorded using a 96-well dual injection luminometer (Tecan). The LUC activity was normalized to the REN activity (LUC/REN). The means and standard errors of LUC/REN were calculated from three independent biological replicates.

Plasmid constructions for the transgenic plants. It has been previously reported that *HAM1*, *HAM2* and *HAM3* are targeted and repressed by the *MIR171* family[19]. To generate new microRNA-sensitive fluorescence reporters for *HAM1*, *HAM2* and *HAM3*, an approach similar to that in a previous report[33] was used. Briefly, a *2×YPET-N7mirS* fragment was generated through PCR amplification, which contains a 2× version of YPET with a N7 nuclear localization sequence (2×YPET-N7) followed by 26 bp of microRNA target sequence (GCAAGGGATATTGGCGCGG CTCAATC) from the *HAM* family. These 26 bp are recognized and targeted by the *MIR171* family[19,34].

For the construction of the *pHAM1::2×YPET-N7mirS* reporter, a 4 kb AscI fragment containing the *HAM1* promoter was amplified from Col-0 genomic DNA with primers 5′-TACA**GGCGCGCC**TTTCCCTCACTTTTTCTTACATT GAA-3′ and 5′-TACA**GGCGCGCC**ACGCCTCCTCAACAACACAGAGTAA-3′ (restriction enzyme sites are in bold), and cloned 5′ of the *2×YPET-N7mirS* fragment. The fused DNA fragment was introduced into the pMOA34 binary vector[35]. For the construction of *pHAM2::2×YPET-N7mirS*, the 3,122 bp *HAM2* promoter was amplified with 5′-TACA**GTTTAAAC**AGCAGGACATATCTAAACCAGA AGTT-3′ and 5′-TACA**GTTTAAAC**GACCAATCTTACAGAGTCAGAAAGA G-3′ (restriction enzyme sites are in bold) and cloned in front of *2×YPET-N7mirS*; and the 1,149 bp *HAM2* 3′ untranslated sequence was PCR amplified with 5′-TAC A**GGCGCGCC**GACGAAAAAGGAGGATATTTTCACGGT-3′ and 5′-TACA**G GCGCGCC**ACTATGTTTCCATGTACTGTGGGATA-3′ (restriction enzyme sites are in bold) and cloned 3′ of the *2×YPET-N7mirS* construct, then the fused DNA fragment was cloned into pMOA34. For the construction of *pHAM3::2×YPET-N7mirS*, the 3,816 bp *HAM3* promoter was amplified with 5′-TACA**GTTTAAAC** TTTATAAGACTTGCTATGGTCGTGAG-3′ and 5′-TACA**GTTTAAAC**TGCA GACGATAAAAAATAGTGTATT-3′ (restriction enzyme sites are in bold) and cloned before *2×YPET-N7mirS*; and the 1,755 bp *HAM3* 3′ untranslated sequence was PCR amplified with 5′-TACA**GGCGCGCC**TTTCCACCGGAGTTTCAATT ATTAAA-3′ and 5′-TACA**GGCGCGCC**TTAGTTGAAGGACAAATAACACCA AA-3′ (restriction enzyme sites are in bold) and cloned 3′ of the *2×YPET-N7mirS* fragment, then the fused DNA fragment was introduced into pMOA34. The double reporter lines, including the *pWUS::DsRed-N7*; *pHAM1::2×YPET-N7mirS* line and the *pWUS::dsRed-N7*; *pHAM2::2×YPET-N7mirS* line, were generated through genetic crosses.

For the construction of the *pHAM4::2×YPET-N7* reporter, the 6,413 bp *HAM4* promoter was amplified with primers 5′-TACA**GGCGCGCC**AAATATAAAAT AGAATCAAACAAAGTTGGTAAC-3′ and 5′-CAAA**GGCGCGCC**GTGTTGT GTGTTAAGAAGAAAGAAAGGTGGAGCCTTT-3′ (restriction enzyme sites are in bold), and cloned 5′ of a *2×YPET-N7* fragment, then the fused DNA fragment was cloned into pMOA34.

For the complementation of *wus-1*, a full-length *WUS* or *WUS* derivative without base pairs encoding amino acids from 203 to 236 was cloned into the pMOA36 binary vector, together with 4.4 kb of the *WUS* upstream regulatory sequence and 1.5 kb of the *WUS* 3′ untranslated sequence. The construct was introduced into *wus-1*/+ plants using the floral dip method. For the complementation of *ham1;2;4*, *HAM1* or the *HAM1* derivative without 117–230 was cloned into the pMOA34 binary vector, with 3,949 bp of the *HAM1* upstream regulatory sequence and 1,387 bp of the *HAM1* 3′ untranslated sequence. The construct was introduced into *ham1;2;4* plants using the floral dip method.

To generate a *MIR171* expression construct in shoot meristems, the *MIR171* DNA was amplified with 5′-CACCTGAGCGCACTATCGGACATCAAA-3′ and 5′-TAAACGCGTGATATTGGCAC-3′ and cloned into pMOA36 together with 4.4 kb of the *WUS* upstream regulatory sequence and 1.5 kb of the *WUS* 3′ untranslated sequence. The construct was introduced into the *ham4* mutant through the floral dip method. Five independent transgenic plants (*pWUS::MIR171* in *ham4*) showing terminated vegetative meristems were identified.

Confocal imaging of fluorescence reporters in living plants. All of the fluorescent reporters were imaged by using a Zeiss LSM 510 Meta confocal microscope, except for the fluorescent reporters in inflorescence meristems and HAM2 fluorescent reporters in the roots, which were imaged by using a Zeiss LSM 780 Meta confocal microscope. Zeiss LSM software was used for reconstructing the *Z*-stacks for a projection view. Laser and filter settings were used as described previously[36–38]. To image *HAM4* and *WOX4* reporters, the cotyledons, first leaf, hypocotyls and roots from 7-day-old seedlings and stems from 1-cm bolting plants were used. To image dsRed, YPET and PI simultaneously in SAMs, the multitracking mode in the ZEISS LSM 780 was used. dsRed was excited using a 561 nm laser line in conjunction with 571–589 nm collection; YPET was excited using a 514 nm laser line in conjunction with a 519–549 nm collection; and PI was excited using a 514 nm laser with 631–673 nm collection. There is no spectral bleed-through of dsRed into the YPET collection channel, nor of YPET into the dsRed collection channel under these settings, and for better display, all images from the dsRed channel were equally enhanced with the same scale and all images from the PI channel were uniformly enhanced to the similar intensity using ImageJ software.

Histology. The wild-type and *ham1;2;3;4* seedlings were fixed in 4% paraformaldehyde, dehydrated and embedded in Paraplast X-tra (Fisher). The samples in wax were sectioned at 8 μm, de-waxed and dehydrated, and the slides were stained with Alcian blue together with Safranin O (red) as previously described[39], to detect non-lignified cell walls and lignified cell walls, respectively.

Real-time RT–PCR analysis. Total RNA was isolated from 10-day-old plants with roots, hypocotyls and leaves dissected off, using the RNeasy Kit (Qiagen). SuperScript III reverse transcriptase (Invitrogen) was used to synthesize the first-strand cDNA with oligo(dT) primer and 1 μg of total RNA at 50 °C for 1 h. Quantitative PCR was then performed with the SensiMix SYBR Hi-ROX Kit (Bioline) on Roche Real-Time PCR machine following the manufacturer's instruction. The thermal cycling program was 95 °C for 10 min, followed by 45 cycles of 95 °C for 10 s, 56 °C for 30 s, 72 °C for 40 s, and a one-cycle dissociation stage at 95 °C for 15 s, 60 °C for 1 min, and 97 °C for 15 s. The primers used in quantitative RT–PCR were: *JAZ5*, 5′-GAAAGACAGAGCTGTGGCTAGG-3′ and 5′-TTGGCCTTCTTCAATCTT CATAATA-3′; *TIP2;2*, 5′-ACCAATGGCGAGAGCGTACCG-3′ and 5′-ATGA AACCGATAGCAATTGGAG-3′; *TCP9*, 5′-ACCTCCTTTACAAGTTGTTCCA AG-3′ and 5′-TGAAGCTCTTGTTTCTCGTATATCTC-3′; *GRP23*, 5′-AGACA GCTAGCCATCAGCAGTCAC-3′ and 5′-AGTTCCTCAACTCCACTACCTTT TT-3′; *TPL*, 5′-AGCTAGTCTCAGCAATTCAAA-3′ and 5′-AGGCTGATCAG ATGCAGAGG-3′; and *UBQ10*, 5′-AACAATTGGAGGATGGTCGT-3′ and 5′-T TCCAGGGAAGATGAGACG-3′. Fold change was calculated as $2^{\Delta\Delta Ct}$ and standard error was calculated from three biological replicates, and each biological replicate was examined in triplicate.

ChIP. For the construction of *pHAM2::YFP-HAM2* (*pHAM2::YPET-HAM2*), the YFP variant YPET was amplified and cloned in front of *HAM2* cDNA in-frame to generate the *YFP-HAM2* fragment. Then the 3,122 bp *HAM2* promoter was amplified with 5′-TACA**GTTTAAAC**AGCAGGACATATCTAAACCAGAAGTT-3′ and 5′-TACA**GTTTAAAC**GACCAATCTTACAGAGTCAGAAAGAG-3′ (restriction enzyme sites are in bold) and cloned in front of *YFP-HAM2*, and the 1,149 bp *HAM2* 3′ untranslated sequence was amplified with 5′-TACA**GGCGCGCC**GAC GAAAAAGGAGGATATTTTCACGGT-3′ and 5′-TACA**GGCGCGCC**ACTAT GTTTCCATGTACTGTGGGATA-3′ and cloned 3′ of *YFP-HAM2*. Then the whole fused DNA fragment (*pHAM2-YFP-HAM2-HAM2 3′UTR*) was cloned into the binary vector pMOA34. The construct was introduced into *ham1;2;4* plants using the floral dip method, and the complemented *ham1;2;4 [pHAM2::YFP-HAM2]* line was selected for the western blot, GFP immunoprecipitation (shown in Extended Data Fig. 6f) and ChIP experiments.

A ChIP followed by a quantitative real-time PCR approach was used to investigate the *in vivo* association of HAM2 with the *TPL* and *GRP23* promoters as described previously[40] with some modifications. In general, 2 g of *ham1;2;4* (negative control) or *ham1;2;4 [pHAM2::YFP-HAM2]* plants were harvested and fixed with 1% formaldehyde under vacuum. Nuclei were isolated and lysed, and chromatin was sheared to an average size of 500 bp by sonication seven times for 20 s each with a Branson Sonifier. Samples were kept on ice during sonication and were cooled for 1 min between sonication pulses. The sonicated chromatin served as input. Immunoprecipitations were performed with GFP–Trap Agarose beads (Chromotek) at 4 °C following the manufacturer's procedure. The precipitated DNA was isolated and purified, and served as a template for PCR. Quantitative PCR was performed as described earlier. The relative enrichment for each immunoprecipitated amplicon (from *TPL* or *GRP23* promoter) from GFP–Trap is presented as ChIP/input ratio, and *TUA4* and *ACTIN7* (*ACT7*) amplicons are also included to serve as negative controls. The ChIP experiments were conducted three times using independent biological replicates with similar results, and one representative data set with two technical replicates is presented. The primer pairs used in ChIP-PCR are as follows: *TPL* amplicon 1, 5′-GCAATTGGCTCTTCAATGTC-3′ and 5′-GGACGGAGAT CTAACGGCTA-3′; *TPL* amplicon 2, 5′-CCATATGACCGGGATATGAGA-3′ and 5′-GGGATATGTCGCTTTCCATT-3′; *TPL* amplicon 3, 5′-TTGAGTCAGG GCTCATCTCC-3′ and 5′-CTTTCGCGAGAACCAACTTC-3′; *GRP23* amplicon 1, 5′-ACCATCGTCATTGGTTTCGT-3′ and 5′-GGAGGTGACTGAGAGACA TGG-3′; *GRP23* amplicon 2, 5′-CAACAAATTCCTGTTTTCACGTT-3′ and 5′-C GAAAATGTTCGAACTGCAT-3′; *GRP23* amplicon 3, 5′-CGCCATCGCCTAA AAGTAAA-3′ and 5′-TTTGTTGGCTAGGCATAGGG-3′; *GRP23* amplicon 4, 5′-AGACAGCTAGCCATCAGCAGTCAC-3′ and 5′-AGTTCCTCAACTCCA CTACCTTTTT-3′; *TUA4* amplicon, 5′-CTTTGGTCTTTAGCAGGTTC-3′ and 5′-CCCATCTGTATATAACGACAC-3′; *ACTIN7* amplicon, 5′-TGCTTGTTAT GTGATTCGATCC-3′ and 5′-GATCGACAGAAGCGAGAAGAAT-3′.

Staining. mPS-PI staining and root imaging of the staining was performed as previously described[41].

Scanning electron microscopy. For scanning electron microscopy, tissue was placed in 1.2% glutaraldehyde in 0.025 M phosphate buffer (sodium phosphate, pH 6.8),

vacuum was applied for 10 min, and tissue was fixed overnight at 4 °C. Tissue was then rinsed twice with 0.025 M phosphate buffer for 1 h, post-fixed with 0.5% osmium tetroxide in 0.025 M phosphate buffer for 24 h at room temperature, and moved through an increasing ethanol series (20% increments), each increment lasting a minimum of 1 h and ending with two exchanges of 100% ethanol. Ethanol was removed by critical point drying with a critical point drier (SAMDRI), and tissue was mounted to stubs with double-sided adhesive tape and sputter coated with gold-palladium alloy using a Hummer Sputtering System (Anatech). Samples were examined with a Hitachi 4700 scanning electron microscope.

Primers used for cDNA clones and deletion constructions. *HAM1c*/5CACC, 5′-CACCATGCCCTTATCCTTTGAAAGGTTTCAAGG-3′; *HAM1c*/3, 5′-ACATTTCCAAGCAGAGACAGTAACAAG-3′; *HAM1c5*/231, 5′-CCGTTTTATCACAACAACCAG-3′; *HAM1c5*/441, 5′-GAAAATCTCAAAACATTCG-3′; *HAM1D71–116*/5, 5′-AGTCCTCTCGCTTCTTATTCTGCTTCTTCTCCTGGTCAAGAGC-3′; *HAM1D71–116*/3, 5′-GCTCTTGACCAGGAGAAGAAGCAGAATAAGAAGCGAGAGGACT-3′; *HAM1c71*/5CACC, 5′-CACCATGTCTACCACCACCACGCTGTCTTCCTCT-3′; *HAM1D117–230*/5, 5′-GATGATCTTGACGGTGTTCTCTCTCCGTTTTATCACAACAACCAGCAA-3′; *HAM1D117–230*/3, 5′-TTGCTGGTTGTTGTGATAAAACGGAGAGAGAACACCGTCAAGATCATC-3′; *HAM4c*/5, 5′-ATGAAAATCCCTGCATCATCTCCTC-3′; *HAM4c*/3, 5′-AAACCGCCAAGCTGATGTGGCAACA-3′; *WUSc5*/1, 5′-ATGGAGCCGCCACAGCATCAG-3′; *WUSc5*/30, 5′-TACACGTGTCGCCAGACCAG-3′; *WUSc5*/100, 5′-AGATTCAACGGAACAAACATGAC-3′; *WUSc5*/171, 5′-GCAAGCTCAGGTACTGAATGT-3′; *WUSc*/3stop, 5′-CTAGTTCAGACGTAGCTCAAGA-3′; *WUSc3*/236, 5′-ACCTTCTAGACCAAACAGAGG-3′; *WUSc3*/292, 5′-GTTCAGACGTAGCTCAAGAGAAGC-3′; *WUSD164–183*/5, 5′-TAACAAGCCATATCCCAGCTTCAATGGCTACATGAGTAGCCATG-3′; *WUSD164–183*/3, 5′-CATGGCTACTCATGTAGCCATTGAAGCTGGGATATGGCTTGTTA-3′; *WUSD101–163*/5, 5′-GGCTCGTGAGCGTCAGAAGAAGAGAAATAACGGGAATTTAAATCATGCAA-3′; *WUSD101–163*/3, 5′-TTGCATGATTTAAATTCCCGTTATTTCTCTTCTTCTGACGCTCACGAGCC-3′; *WUSD132–163*/5, 5′-TATCATCCTCTACTTCACCATCATAATAACGGGAATTTAAATCATGCAA-3′; *WUSD132–163*/3, 5′-TTGCATGATTTAAATTCCCGTTATTATGATGGTGAAGTAGAGGATGATA-3′; *WUSD184–236*/5, 5′-AATGTGGTGTTGTTAATGCTTCTCATCAAGAAGAAGAAGAATGTGG-3′); *WUSD184–236*/3, 5′-CCACATTCTTCTTCTTCTTGATGAGAAGCATTAACAACACCACATT-3′; *WUSD164–236*/5, 5′-TAACAAGCCATATCCCAGCTTCCATCAAGAAGAAGAAGAATGTG-3′; *WUSD164–236*/3, 5′-CACATTCTTCTTCTTCTTGATGGAAGCTGGGATATGGCTTGTTA-3′; *WUSD184–202*/5, 5′-AATGTGGTGTTGTTAATGCTTCTTACAACAACGTAGGTGGAGGAT-3′; *WUSD184–202*/3, 5′-ATCCTCCACCTACGTTGTTGTAAGAAGCATTAACAACACCACATT-3′; *WUSD203–236*/5, 5′-TGGAACAAGACTGTTCTATGAATCATCAAGAAGAAGAAGAATGTGG-3′; *WUSD203–236*/3, 5′-CCACATTCTTCTTCTTCTTGATGATTCATAGAACAGTCTTGTTCCA-3′; *WUSD218–236*/5, 5′-GGGCAAACATGGATCATCATTACCATCAAGAAGAAGAAGAATGTGG-3′; *WUSD218–236*/3, 5′-CCACATTCTTCTTCTTCTTGATGGTAATGATGATCCATGTTTGCCC-3′; *WUSD203–217*/5, 5′-TGGAACAAGACTGTTCTATGAATTCATCTGCACCTTACAACTTCTT-3′; *WUSD203–217*/3, 5′-AAGAAGTTGTAAGGTGCAGATGAATTCATAGAACAGTCTTGTTCCA-3′; *WOX4c*/5CACC, 5′-CACCATGAAGGTTCATGAGTTTTCGAA-3′; *WOX4c*/3stop, 5′-TCATCTCCCTTCAGGATGGAGAGGA-3′; *WOX5c*/5CACC, 5′-CACCATGTCTTTCTCCGTGAAAGGTC-3′; *WOX5c*/3, 5′-AAGAAAGCTTAATCGAAGATCT-3′; *TomatoHAM*/5CACC, 5′-CACCATGATTGTAATACCTCAAAGTAATAA-3′; *TomatoHAM*/3stop, 5′-TTAAAAGAAAATCTCTTCTGGCTTCAGA-3′; *TomatoWUS*/5CACC, 5′-CACCATGGAACATCAACACAACATAGAAGA-3′; *TomatoWUS*/3stop, 5′-TTAGGGGAAAGAGTTGAGAGTAAGT-3′; *TomatoWOX4*/5CACC, 5′-CACCATGTACATGGGATCATCATCAGGAAG-3′; *TomatoWOX4*/3stop, 5′-TCATCTCATGCCTTCTGGATGCAATG-3′.

24. Fletcher, J. C., Brand, U., Running, M. P., Simon, R. & Meyerowitz, E. M. Signaling of cell fate decisions by CLAVATA3 in *Arabidopsis* shoot meristems. *Science* **283,** 1911–1914 (1999).
25. Gordon, S. P., Chickarmane, V. S., Ohno, C. & Meyerowitz, E. M. Multiple feedback loops through cytokinin signaling control stem cell number within the *Arabidopsis* shoot meristem. *Proc. Natl Acad. Sci. USA* **106,** 16529–16534 (2009).
26. Walter, M. *et al.* Visualization of protein interactions in living plant cells using bimolecular fluorescence complementation. *Plant J.* **40,** 428–438 (2004).
27. Voinnet, O., Rivas, S., Mestre, P. & Baulcombe, D. An enhanced transient expression system in plants based on suppression of gene silencing by the p19 protein of tomato bushy stunt virus. *Plant J.* **33,** 949–956 (2003).
28. Ohashi-Ito, K. & Bergmann, D. C. *Arabidopsis* FAMA controls the final proliferation/differentiation switch during stomatal development. *Plant Cell* **18,** 2493–2505 (2006).
29. Curtis, M. D. & Grossniklaus, U. A gateway cloning vector set for high-throughput functional analysis of genes in planta. *Plant Physiol.* **133,** 462–469 (2003).
30. Pierce, N. W. *et al.* Cand1 promotes assembly of new SCF complexes through dynamic exchange of F box proteins. *Cell* **153,** 206–215 (2013).
31. Harper, S. & Speicher, D. W. Expression and purification of GST fusion proteins. *Curr. Protoc. Protein Sci.* Chapter 6, Unit 6.6 (2008).
32. Huang, X. *et al.* Arabidopsis FHY3 and HY5 positively mediate induction of *COP1* transcription in response to photomorphogenic UV-B light. *Plant Cell* **24,** 4590–4606 (2012).
33. Carlsbecker, A. *et al.* Cell signalling by microRNA165/6 directs gene dose-dependent root cell fate. *Nature* **465,** 316–321 (2010).
34. Wang, L., Mai, Y. X., Zhang, Y. C., Luo, Q. & Yang, H. Q. MicroRNA171c-targeted *SCL6-II*, *SCL6-III*, and *SCL6-IV* genes regulate shoot branching in *Arabidopsis*. *Mol. Plant* **3,** 794–806 (2010).
35. Barrell, P. J. & Conner, A. J. Minimal T-DNA vectors suitable for agricultural deployment of transgenic plants. *Biotechniques* **41,** 708–710 (2006).
36. Heisler, M. G. *et al.* Patterns of auxin transport and gene expression during primordium development revealed by live imaging of the *Arabidopsis* inflorescence meristem. *Curr. Biol.* **15,** 1899–1911 (2005).
37. Reddy, G. V. & Meyerowitz, E. M. Stem-cell homeostasis and growth dynamics can be uncoupled in the *Arabidopsis* shoot apex. *Science* **310,** 663–667 (2005).
38. Sugimoto, K., Jiao, Y. & Meyerowitz, E. M. *Arabidopsis* regeneration from multiple tissues occurs via a root development pathway. *Dev. Cell* **18,** 463–471 (2010).
39. Roeder, A. H., Ferrandiz, C. & Yanofsky, M. F. The role of the REPLUMLESS homeodomain protein in patterning the *Arabidopsis* fruit. *Curr. Biol.* **13,** 1630–1635 (2003).
40. Bowler, C. *et al.* Chromatin techniques for plant cells. *Plant J.* **39,** 776–789 (2004).
41. Truernit, E. *et al.* High-resolution whole-mount imaging of three-dimensional tissue organization and gene expression enables the study of phloem development and structure in *Arabidopsis*. *Plant Cell* **20,** 1494–1503 (2008).

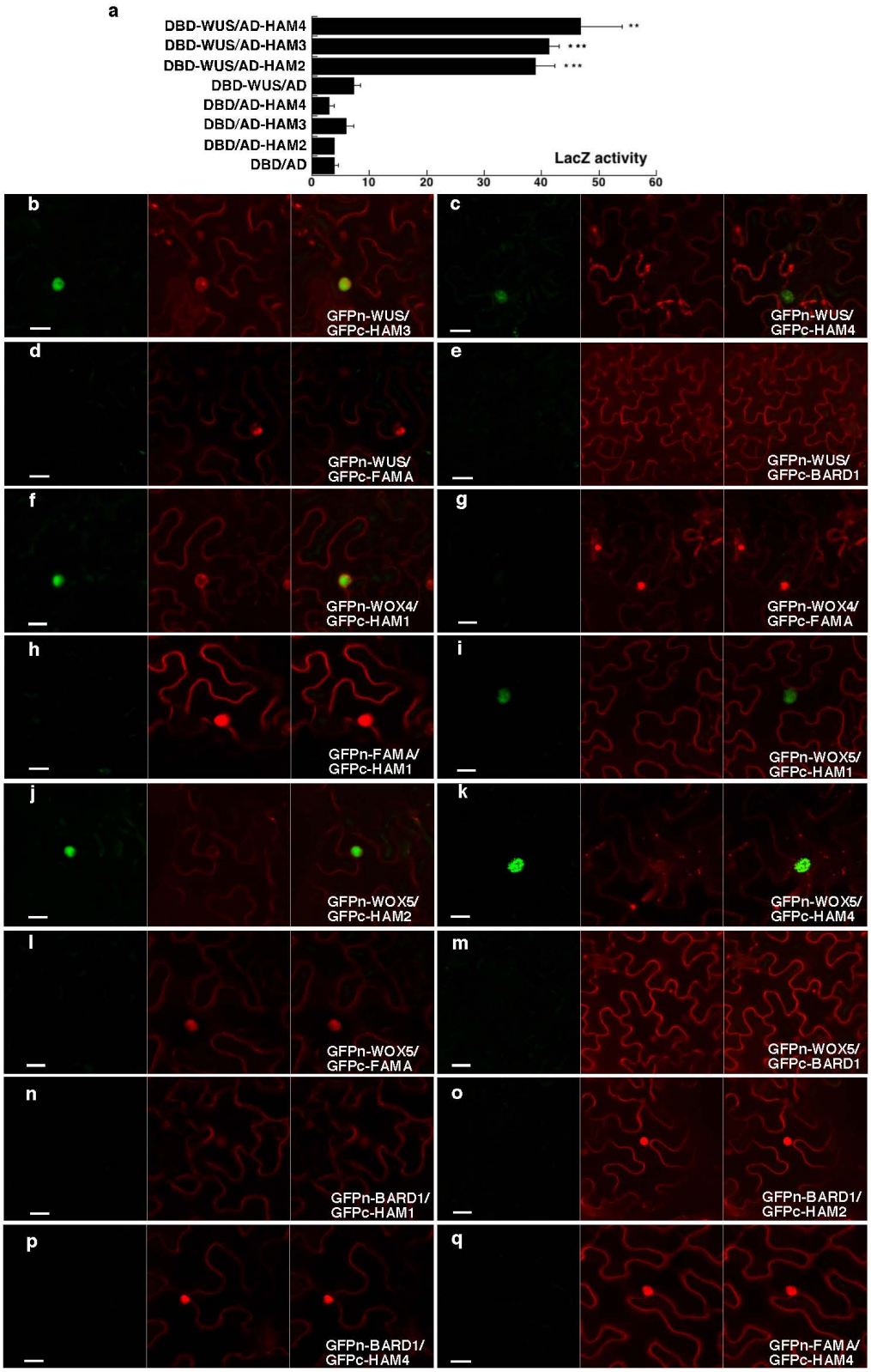

Extended Data Figure 1 | Interaction between WUS/WOX and HAM family transcriptional regulators. **a**, LacZ activity in yeast-two-hybrid assays testing interactions between WUS and HAM2, HAM3 or HAM4. Error bars show mean ± s.e.m. ($n = 3$ biological replicates). $^{**}P < 0.01$; $^{***}P < 0.001$ (two-tailed *t*-test, compared with DBD-WUS/AD). **b**–**o**, BiFC analyses in tobacco transient assays with *HAM* and *WOX* family genes. **c**–**q**, Tobacco was co-transformed with GFPn–WUS and GFPc–HAM3 (**b**), GFPn–WUS and GFPc–HAM4 (**c**), GFPn–WUS and GFPc–FAMA (**d**), GFPn–WUS and GFPc–BARD1 (**e**), GFPn–WOX4 and GFPc–HAM1 (**f**), GFPn–WOX4 and GFPc–FAMA (**g**), GFPn–FAMA and GFPc–HAM1 (**h**), GFPn–WOX5 and GFPc–HAM1 (**i**), GFPn–WOX5 and GFPc–HAM2 (**j**), GFPn–WOX5 and GFPc–HAM4 (**k**), GFPn–WOX5 and GFPc–FAMA (**l**), GFPn–WOX5 and GFPc–BARD1 (**m**), GFPn–BARD1 and GFPc–HAM1 (**n**), GFPn–BARD1 and GFPc–HAM2 (**o**), GFPn–BARD1 and GFPc–HAM4 (**p**), or GFPn–FAMA and GFPc–HAM4 (**q**). BARD1 and FAMA proteins are both included as negative controls. Left panel: GFP channel; middle panel: propidium iodide (PI) staining channel; right panel: merged channels. Scale bars, 20 μm.

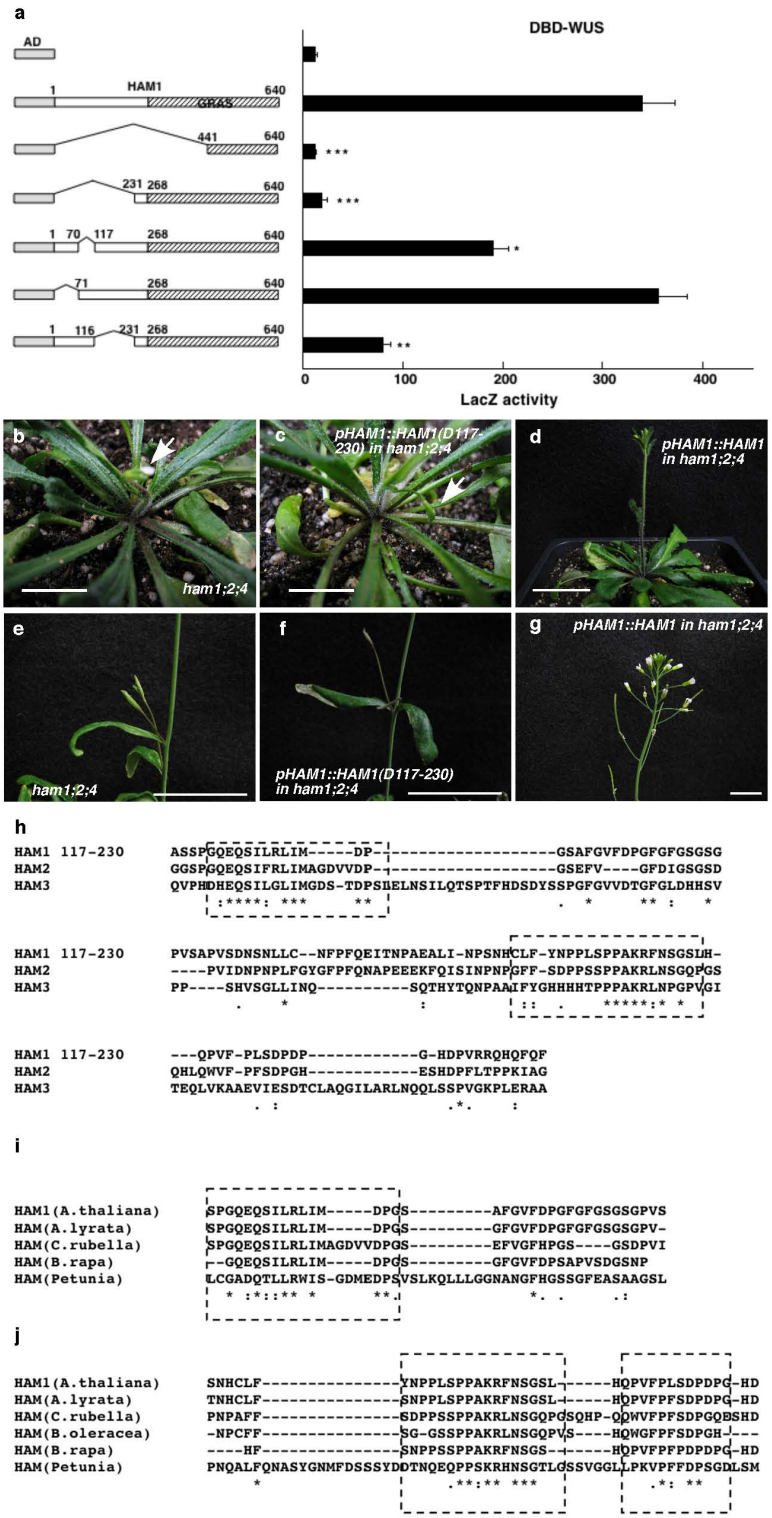

Extended Data Figure 2 | An N-terminal region of HAM1 is important for WUS–HAM1 interaction and is essential for HAM1 function in stem cell maintenance. **a**, Yeast two-hybrid assay of interactions between WUS and various deleted derivatives of HAM1. Deleting amino acids 117 to 230 (D117–230) from HAM1 compromised the WUS–HAM1 interaction. Left, box diagrams of the HAM1 derivatives. Shaded boxes indicate the GRAS domains. Numbers indicate amino acid residues. Error bars show mean ± s.e.m. ($n = 3$ biological replicates). $^{*}P < 0.05$, $^{**}P < 0.01$, $^{***}P < 0.001$ (two-tailed t-test, compared with full-length AD-HAM1). **b**–**g**, The complementation of the *ham1;2;4* triple mutant requires amino acids 117–230. The early termination phenotype of *ham1;2;4* (**b**, **e**) was not complemented by HAM1(D117–230) driven by a *HAM1* promoter and 3′ untranslated region (UTR) (**c**, **f**), but was fully complemented by wild-type *HAM1* (**d**, **g**). **b**, **c**, Arrows indicate the early terminated inflorescences. **h**–**j**, Amino acid sequence alignment of the HAM1 N-terminal domains (117–230) using Clustal Omega. **h**, Sequence alignment of the N-terminal domains among three *Arabidopsis* HAM members. **i**, Sequence alignment of partial N-terminal domains in HAM from *A. thaliana*, *A. lyrata*, *Capsella rubella*, *Brassica rapa* and *Petunia*. **j**, Sequence alignment of partial HAM1 N-terminal domains in HAM from *A. thaliana*, *A. lyrata*, *C. rubella*, *B. oleracea*, *B. rapa* and *Petunia*. Asterisks indicate amino acids that are the same; dots indicate similar amino acids. The conserved regions are boxed. Scale bars: 10 mm (**b**, **c**, **g**); 40 mm (**d**); 20 mm (**e**, **f**).

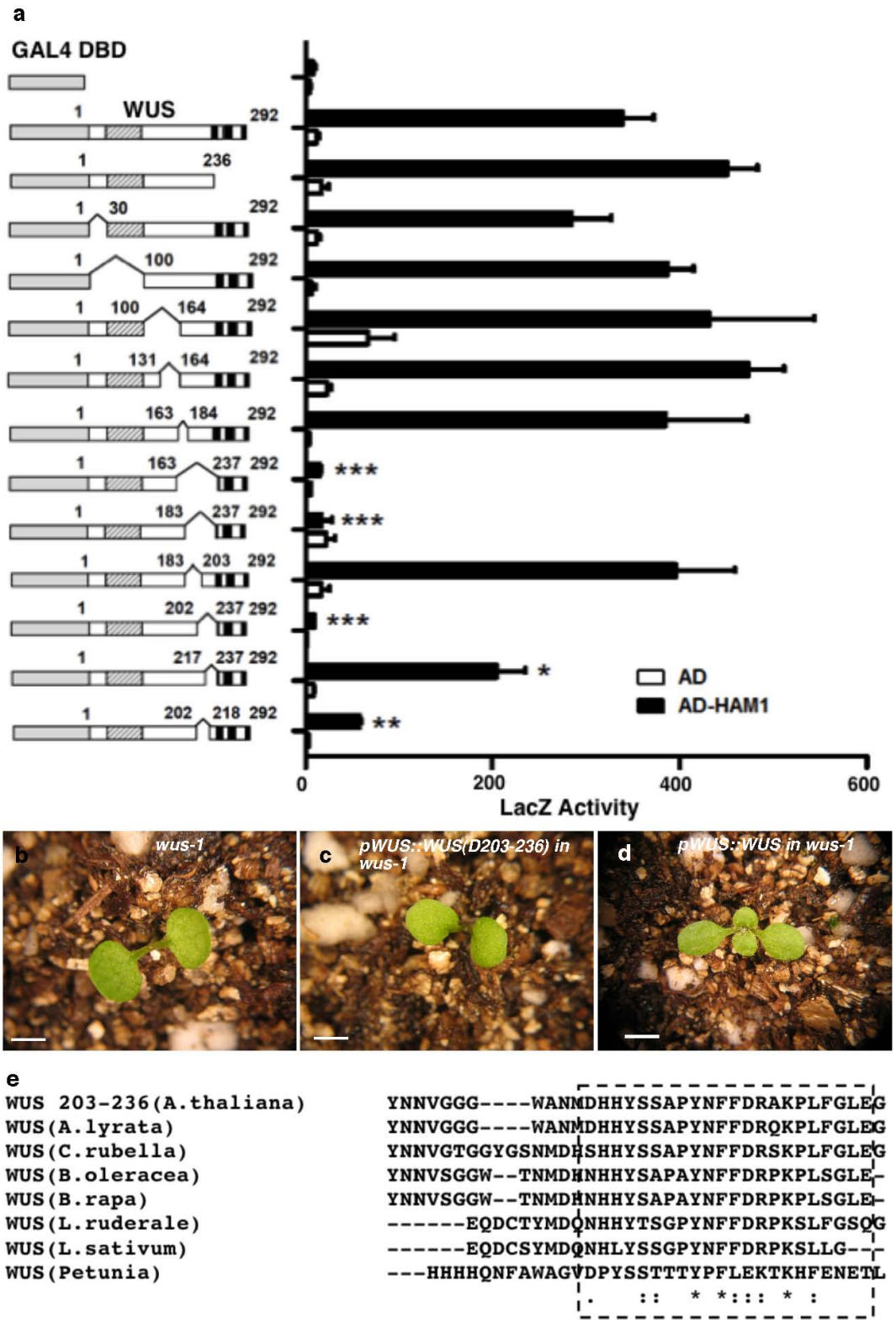

Extended Data Figure 3 | A C-terminal region of WUS is important for WUS–HAM1 interaction and is essential for WUS function in stem cell maintenance. **a**, Yeast-two-hybrid assay of interactions between HAM1 and various deleted WUS derivatives. Deleting amino acids 203 to 236 (D203–236) from WUS greatly compromised the WUS–HAM1 interaction. Left, box diagrams of the deleted WUS derivatives. Shaded boxes indicate the homeodomain; the three black boxes indicate the acidic domains, the WUS box and the EAR motif, respectively. Numbers indicate amino acid residues. Error bars show mean ± s.e.m. ($n = 3$ biological replicates). $^{*}P < 0.05$, $^{**}P < 0.01$, $^{***}P < 0.001$ (two-tailed t-test, compared with DBD-WUS full-length). **b**–**d**, WUS function requires the same region that is important for WUS–HAM1 interaction. The terminated shoot meristem phenotype of *wus-1* (**b**) was not complemented by WUS(D203–236) driven by the *WUS* promoter and 3′ UTR (**c**), and was fully complemented by the wild-type *WUS* (**d**). **e**, Amino acid sequence alignment of C-terminal regions of WUS from *A. thaliana*, *A. lyrata*, *C. rubella*, *B. oleracea*, *B. rapa*, *Lepidium ruderale*, *L. sativum* and *Petunia*, using Clustal Omega. Asterisks indicate amino acids that are the same; dots indicate similar amino acids. The conserved regions are boxed. Scale bars, 2 mm (**b**–**d**).

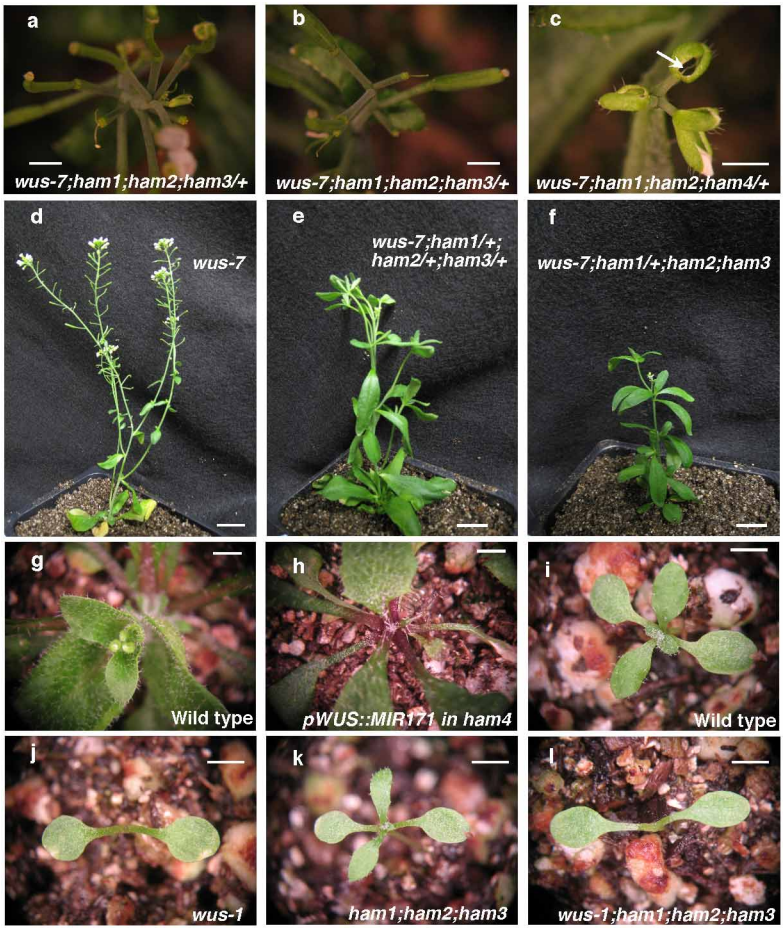

Extended Data Figure 4 | Genetic interaction between WUS and HAM family members. **a**, **b**, The secondary inflorescence meristems initiated from axillary meristems in *wus-7;ham1;2* homozygotes with *ham3*/+ terminate prematurely. **c**, *wus-7;ham1;2* homozygotes with *ham4*/+ display early termination of the main inflorescence meristem and lack of carpels in flowers (indicated by arrow). **d**–**f**, *WUS* and *HAM* family members interact genetically in a dose-dependent manner. *wus-7* (**d**) formed functional shoot apices and normal stature, but *wus-7; ham1/+; ham2/+; ham3/+* (**e**) enhanced the *wus-7* phenotype, and *wus-7; ham1/+; ham2; ham3* (**f**) showed stronger enhancement, with reduced flower numbers and plant stature, and an elongated vegetative stage, resembling a *wus* strong allele. Plants are at 36 days after germination. **g**, **h**, Downregulation of *HAM1*, *HAM2* and *HAM3* in *ham4* shoot meristems leads to an early termination phenotype. Compared to wild type (Col) (**g**), *pWUS::MIR171* in *ham4* (**h**) showed terminated vegetative meristems. **i**–**l**, WUS is required for the functions of HAM1, HAM2 and HAM3. At 11 days after germination, compared with Ler wild type (**i**) and *ham1;2;3* (**k**), which formed functional vegetative meristem and leaf primordia, *wus-1; ham1;2;3* (**l**) displays terminated vegetative meristems similar to *wus-1* (**j**). Scale bars, 2 mm.

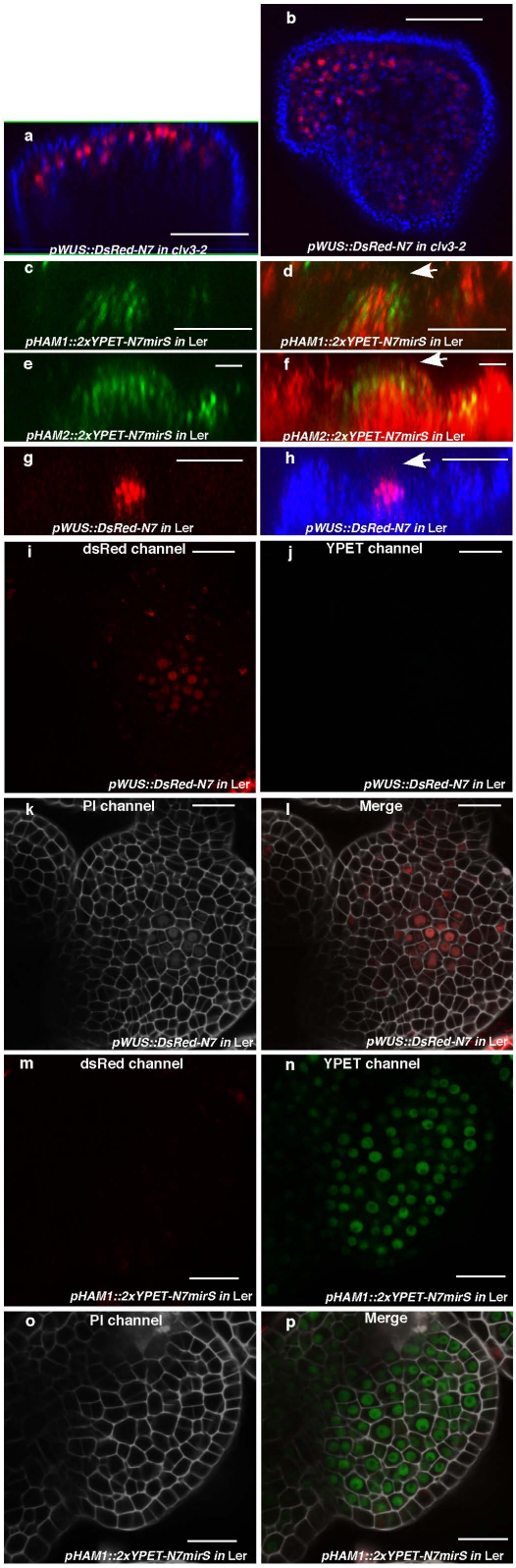

Extended Data Figure 5 | Expression of *HAM1*, *HAM2* and *WUS* in the SAMs. **a**, **b**, *WUS* expression in *clv3-2*. Orthogonal (**a**) and top (**b**) views of *pWUS::DsRed-N7* expression (red) and chlorophyll autofluorescence (blue) in the same *clv3-2* inflorescence meristem. **c**–**h**, Comparison between expression patterns of *HAM1*, *HAM2* and *WUS* in vegetative meristems. **c**, Orthogonal view of *pHAM1::2×YPET-N7mirS* expression (green) in Ler vegetative meristem. **d**, Orthogonal view of *pHAM1::2×YPET-N7mirS* expression (green) together with chlorophyll autofluorescence (red) in the same vegetative meristem shown in **c**, indicating that *HAM1* is expressed in the rib meristem. **e**, Orthogonal view of *pHAM2::2×YPET-N7mirS* expression (green) in Ler vegetative meristem. **f**, Orthogonal view of *pHAM2::2×YPET-N7mirS* expression (green) together with chlorophyll autofluorescence (red) in the same vegetative meristem shown in **e**, indicating that *HAM2* is highly expressed in the rib meristem. **g**, Orthogonal view of *pWUS::DsRed-N7* expression (red) in Ler vegetative meristem. **h**, Orthogonal view of *pWUS::DsRed-N7* expression (red) together with chlorophyll autofluorescence (blue) in the same vegetative meristem shown in **g**, indicating that *WUS* is expressed in the rib meristem. Arrows indicate the positions of the L1 cell layer. **i**–**p**, Control images confirming the specificity of confocal spectral settings for Fig. 3 (**e**–**l**). The SAMs from the *pWUS::DsRed-N7* line (**i**–**l**) or *pHAM1::2×YPET-N7mirS* line (**m**–**p**) were imaged from the same three separated channels used in Fig. 3 (**e**–**l**). There is no spectral bleed-through of YPET signal into the dsRed channel (**m**), nor dsRed signal into the YPET channel (**j**). **i**, **m**, dsRed channel (red); **j**, **n**, YPET channel (green); **k**, **o**, PI staining channel (grey); **l**, **p**, merged all three channels. Scale bars: 50 μm (**a**–**d**, **g**, **h**); 20 μm (**e**, **f**, **i**–**p**).

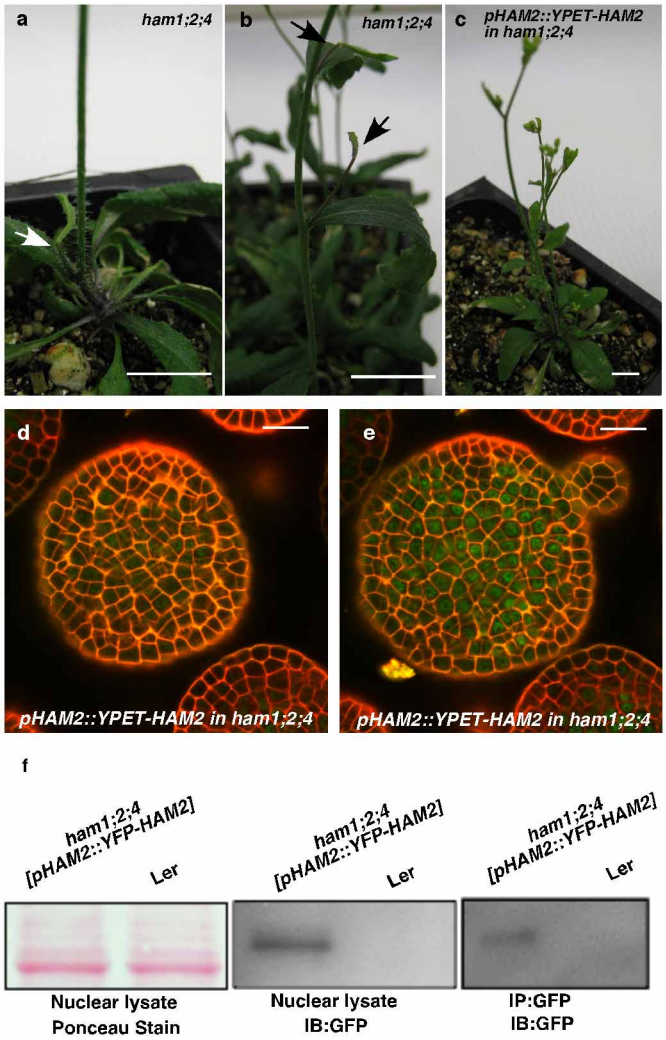

Extended Data Figure 6 | *pHAM2::YFP-HAM2* (*pHAM2::YPET-HAM2*) complemented the *ham1;2;4* mutant and was expressed in the centre of SAMs. **a**–**c**, The early termination phenotype of *ham1;2;4* (**a**, **b**) was completely complemented by YPET–HAM2 driven by the *HAM2* promoter and 3′ UTR (**c**), indicating that the promoter used for HAM2 transcriptional and translational reporters is functional and that the fusion protein (YPET–HAM2) is also functional *in vivo*. **a**, **b**, Arrows indicate early terminated apices. **a**–**c**, Scale bars, 10 mm. **d**, **e**, Different *Z* sections from the same SAM from a *ham1;2;4 [pHAM2::YPET-HAM2]* plant depicted in Fig. 3m, n shows expression of *pHAM2::YPET-HAM2* translational marker (green) in L2 (**d**) and L3 (**e**), together with PI as counter stain (red). **d**, **e**, Scale bars, 20 µm. **f**, Immunoblot with anti-GFP antibody validates the presence of YFP–HAM2 (YPET–HAM2) in both nuclear lysate and nuclear proteins immunoprecipitated with GFP–Trap from *ham1;2;4* [*pHAM2::YFP-HAM2*] line used in ChIP experiment (Fig. 2n, o). IB, immunoblot; IP, immunoprecipitation.

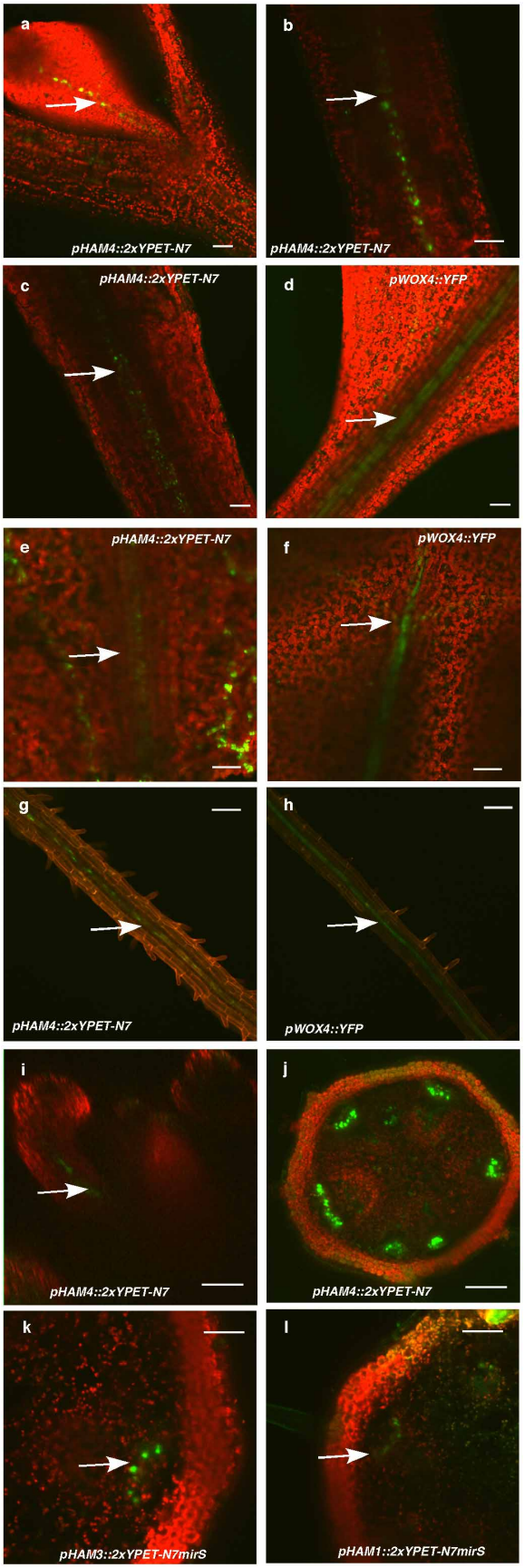

Extended Data Figure 7 | Expression patterns of *HAM* genes in comparison with *WOX4*. **a**, *pHAM4::2×YPET-N7* (green, indicated by arrow) is expressed in procambium cells of the first leaf. **b**, *pHAM4::2×YPET-N7* (green, indicated by arrow) is expressed in vasculature in the 7-day-old hypocotyl. **c**–**h**, Comparison of *pHAM4::2×YPET-N7* (green, indicated by arrow) and *pWOX4::YFP* (green, arrow indicated) expression patterns in vasculature cells in the 7-day-old leaf petiole (**c**, **d**), 20-day-old leaf petiole (**e**, **f**) and 7-day-old root (**g**, **h**). **i**, Orthogonal view of *pHAM4::2×YPET-N7* (green, indicated by arrow) expression in flower vasculature. **j**, Procambium-specific expression of *pHAM4::2×YPET-N7* in stems from 1-cm bolting plants. **k**–**l**, Procambium-specific expression of *pHAM3::2×YPET-N7mirS* (**k**) and *pHAM1::2×YPET-N7mirS* (**l**) in transverse sections of stems from 1-cm bolting plants. Red represents chlorophyll autofluorescence (**a**–**f**, **i**–**l**), or PI staining (**g**, **h**). Scale bars: 50 μm (**a**, **h**–**i**, **k**–**l**); 100 μm (**b**–**g**, **j**).

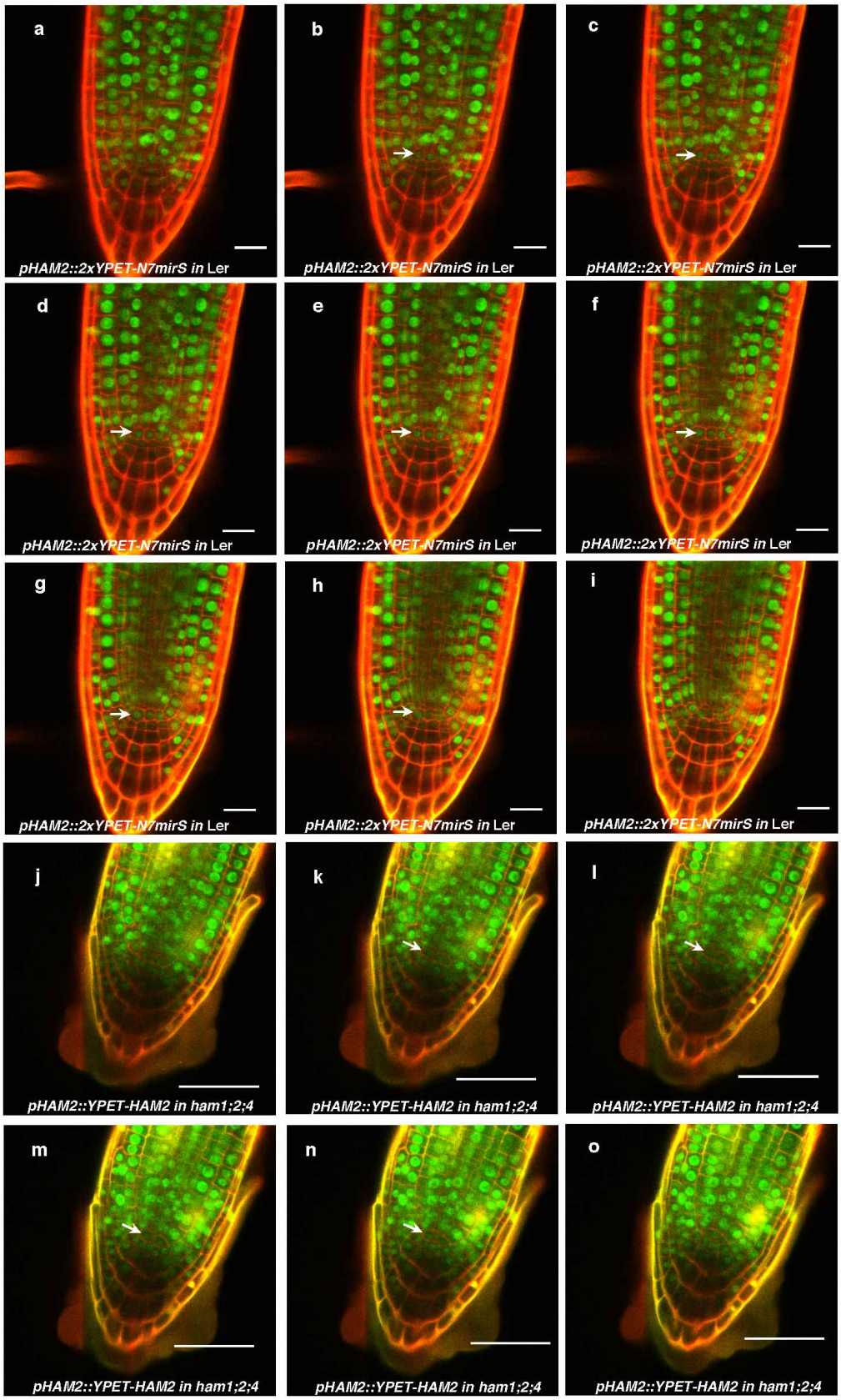

Extended Data Figure 8 | Expression patterns of *HAM2* transcriptional and translational reporters in root meristems. **a**–**i**, Complete stacks of confocal sections through the root tip demonstrate that *pHAM2::2×YPET-N7mirS* (green) is expressed in the quiescent centre cells (indicated by arrow) and in cells above the quiescent centre within the root meristem. **j**–**o**, Expression patterns of HAM2 translational reporters in *ham1;2;4* root meristems. Complete stacks of confocal sections through the root tip demonstrate that *pHAM2:YPET-HAM2* (green) is present in the quiescent centre cells (indicated by arrows) and the cells above the quiescent centre within the root meristem in the *ham1;2;4* mutant. Cellular outlines were stained with PI (red). Scale bars: 20 μm (**a**–**i**); 50 μm (**j**–**o**).

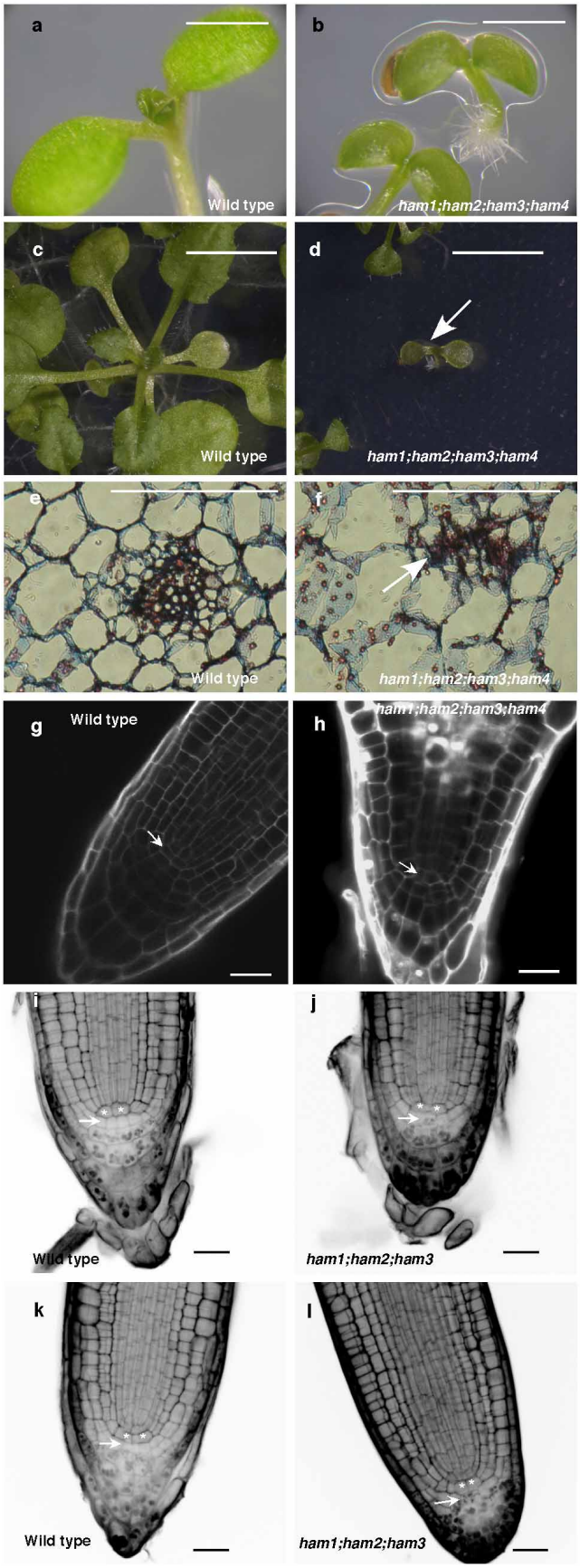

Extended Data Figure 9 | HAM family regulates various stem cell niches. **a**–**d**, Growth arrest of *ham1;2;3;4* at the seedling stage. **a**, **b**, Imaging of Ler wild-type (**a**) and homozygous *ham1;2;3;4* (**b**) seedlings at 7 DAG. **c**, **d**, Imaging of wild-type (**c**) and homozygous *ham1;2;3;4* (**d**) (indicated by arrow) seedlings at 26 DAG. **e**, **f**, Transverse section of leaves from wild-type (**e**) and *ham1;2;3;4* (**f**) at 7 DAG. **f**, Arrow indicates undifferentiated/undetermined cell mass. **g**, **h**, Confocal imaging of root meristem from wild-type (**g**) and *ham1;2;3;4* (**h**) seedlings at 7 DAG. *ham1;2;3;4* displayed enlarged cells with abnormal shapes at the quiescent centre (indicated by arrows) and CSC positions. **g**, **h**, Cellular outlines were visualized with PI staining (white). **i**–**l**, mPS-PI[41] stains indicate that *HAM* genes regulate root cell differentiation. Some CSCs (arrow indicated) undergo differentiation with starch accumulated and stained in homozygous *ham1;2;3* (**j**, **l**), but none of them can be stained in Ler wild type (**i**, **k**). Asterisks mark the quiescent centre cells. Scale bars: 5 mm (**c**, **d**); 1 mm (**a**, **b**, **e**, **f**), 20 μm (**g**–**l**).

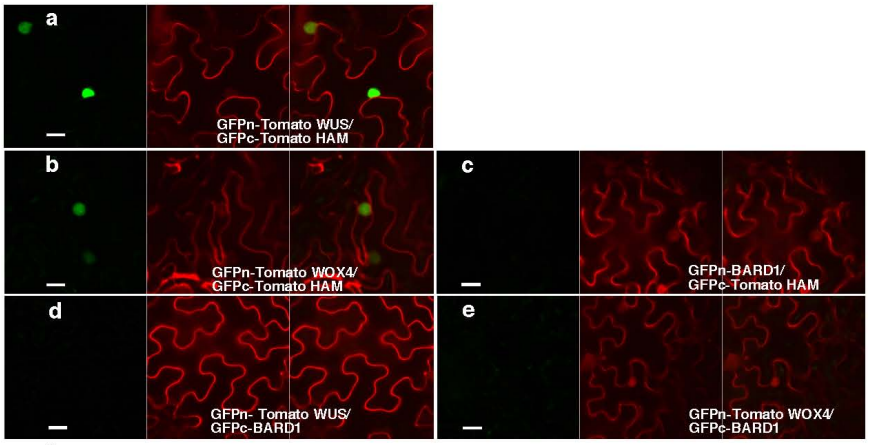

f

```
AtHAM1          ---MPLSFERFQGEGVFGLSSSSFYS---------------DSQKIWSNQDKTEAKQEDL    42
PetuniaHAM      MIAIPQ-----GAKGVLGVSSFMPSISSEEQICKKDANFARNDPQICKKDGNFARNEPQI    55
TomatoHAM       MIVIPQ-SNNLPAKGVLGVSGFVPSISSSS-------------------------SPEASI    35
                   :*       .:**:*:*.                                    : .:

AtHAM1          GYVVGGFL-PEPTSVLDALRSPSPLASYSSTTTTLSSSHGGGGTTVTNTTVT--AGD---    96
PetuniaHAM      CKKEGNFTRNEPVSVLD-TRSPSPSS--SS--CSYA---------------GKVEGQKEE    95
TomatoHAM       CKKDANFTRNEPVSVLD-TRSPSPSASSSS--CSYGAQHGGN-TAVPGVGSGKTDGRKEE    91
                     . *   **.****  ***** :  **   : .                    *

AtHAM1          ----------DNNNNKCSQMGLDDLDGVLSASSPGQEQSILRLIMDP----GSAF-----   137
PetuniaHAM      LVKELQPFPLVGLEPEKCSLGFGDLDNLLPEL-CGADQTLLRWISGDMEDPSVSLKQLLL   154
TomatoHAM       LVTELEPFT-VGLEPEKSVLGFGDLDNLLPEF-AGSDQSFLRWISGDVEDPSVSLKQLLN   149
                              : : . :*: *** :*     * :*::** *        . ::

AtHAM1          GVFDPGFGFGSGSGPVSAP----VSDN-----SNLLCNFPFQEITNPAEALINPSN----   184
PetuniaHAM      GGNANGF-HGSSGFEASAAGSLVHTDNVSFSGSDVSLNANIEKIGSVIDSNGRPSNGFDY   213
TomatoHAM       GDLGCGVSLQSSGFEVSATGSLAHSDNVSFSGSNICLNANIEKLSSVIDSINSRNNNFEN   209
                *    *.   *..  .**       :**     *::  *  :::: .  ::    .*

AtHAM1          ------------------------------------HCLFY---------------NPP   192
PetuniaHAM      LNANLYAKSLPLPPASSFQEQKLGQKPQSFS----PNQALFQNASYGNMFDSSSYDDTNQ   269
TomatoHAM       PNVNP----------------SLEQKPQPFGPQVMANQTQFQNAACVNIFGSSSYD-INQ   252
                                                  :  *

AtHAM1          LSPPAKRFNSGSLHQPVFPLSDPDPGHDP-----VRRQH----QFQFPFYHNNQQQQFPS   243
PetuniaHAM      EQPPSKRHNSGTLGSSVGGLLPKVPFFDPSGDLSMRRQLLGEMQQHFNLLPPQQFQPKPL   329
TomatoHAM       EQPPPKRHNSGTLG---GALLPKVPFFDANCDFMLRKQPLGQMQPQVNLLPPHQFQPKPL   309
                 .** **.***:*      *    * .*      :*:*     * :. :   .* *  *

AtHAM1          ----SSSSTAVAMVPVPSPGMAGDDQSVIIEQLFNAAELIGTTGNNNGDHTVLAQGILAR   299
PetuniaHAM      IVPKLEAACGGGNGSLMVPRHQQQEQQFIYDQIFQASELLLAG------HFSNAQMILAR   383
TomatoHAM       IVPKLEAAGGGGNGNLMVPRHQLQEQQFIYDQIFQASELLLAG------QFSNAQMILAR   363
                     .:: . .   :  *    ::*..* :*:*:*:**: :       :   ** ****

AtHAM1          LNHHLNTSSNHKSPFQRAASHIAEALLS-----LIHNESSPPLITPENLILRIAAYRSFS   354
PetuniaHAM      LNQQLSP---IGKPFKRAAFYFKEALQLPFLLPCTSTFLPPRSPTPFDCVLKMDAYKSFS   440
TomatoHAM       LNQQLSP---IGKPSRRAAFYIKEALQLPFLLPCTSTFLPPRSPTPFDCVLKMDAYKAFS   420
                **::*.      .* :*** :: ***          .   *   ** : :*:: **::**

AtHAM1          ETSPFLQFVNFTANQSILESCNESGFDRIHIIDFDVGYGGQWSSLMQELASGVGGRRRNR   414
PetuniaHAM      EVSPLIQFMNFTSNQAILEALG--DVERIHIIDFDIGFGAQWSSFMQELPSSN-----RK   493
TomatoHAM       EISPLIQFMNFTSNQAILEALG--DAEQIHIIDFDIGFGAQWSSFMQELPSSN-----RK   473
                * **::**:***:**:***:      ::*******:*:*.****:**** *.      .:

AtHAM1          ASSLKLTVFAPPPSTVSDEFELRFTEENLKTFAGEVKIPFEIELLSVELLLNPAYWPLSL   474
PetuniaHAM      ATSLKITAFASPSTHH--SVEIAIMHESLTQFANDAGIRFELEVINLDTFDPKSYPLSSL   551
TomatoHAM       ATSLKITAFASPSTHH--SIEIGIMHESLTQFANDAGIRFELEVINLDSFDPKSYPLSTL   531
                *:***:*.** * :    ..*: : .*.*. ** :. * **:*::.:: :   :*   :*

AtHAM1          RSSEKEAIAVNLPVNSVASGY--LPLILRFLKQLSPNIVVCSDRGCDRNDAPFPNAVIHS   532
PetuniaHAM      RSSDCEAIAINFPIWSISSCLFAFPSLLHYMKQLSPKIIVSLERGCERTELPLKHHLLHA   611
TomatoHAM       RSSECEAIAINFPIWSISSCPFAFPSLLHCMKQLSPKVVVSLERGCERTELPLKHHLIHA   591
                ***: ****:*:*: *::*    :* :*: :*****:::*. :***:*.: *: . ::*:

AtHAM1          LQYHTSLLESLDANQNQD--DSSIERFWVQPSIEKLLMKRHRWIERSPPWRILFTQCGFS   590
PetuniaHAM      LQYYEILLASIDAANVTPEIGKKIEKSLLLPSIENMVLGRLRSPDRMPQWRNLFASAGFS   671
TomatoHAM       LQYYETLLASIDAANITPDIGKKIERSLFQPSIENMILGRLRSSDRMPPWRNLFASAGFS   651
                ***:  ** *:** :      ..**:  . ****:::: * *  :* * ** **:..***

AtHAM1          PASLSQMAEAQAECLLQRNPVRGFHVEKRQSSLVMCWQRKELVTVSAWKC----------   640
PetuniaHAM      PVAFSNLTEIQAECVVKRTQVGGFHVEKRQSSLVLCWKQQELLSALTWRC----------   721
TomatoHAM       PVAFSNMTEIQAECVVKRTQVGGFHVQKRQTSLVLCWKQQELLSAVTWRCRGAFLLKPEE   711
                *.::*:::* ****:::*. * ****:***:***:**:::**::. :*:*
```

Extended Data Figure 10 | Interaction between WOX and HAM homologues from tomato (*Solanum lycopersicum*). **a**, **b**, **f**, BiFC analyses in tobacco transient assays demonstrated that tomato WUS (NCBI gene accession number 543793) physically interacted with a putative tomato HAM homologue (sequence accession number: LEFL2052P11 from Kazusa Full-length Tomato cDNA database) (**a**) identified based on its sequence homology to HAM from *Arabidopsis* and *Petunia* (**f**), and that tomato WOX4 (ref. 10) (NCBI gene accession number 100301933) physically interacted with the putative tomato HAM homologue (**b**). **c**–**e**, BARD1 protein is included as a negative control. Left panel: GFP channel; middle panel: PI staining channel; right panel: merged channels. Scale bars, 20 μm. **f**, Amino acid sequence alignment of a putative tomato HAM, *Arabidopsis* HAM1 and *Petunia* HAM using Clustal Omega. Asterisks indicate amino acids that are the same; dots indicate similar amino acids.